Supplemental Information

Supplemental Experimental Procedures

Algorithms tested with ExCoR

An algorithm describes an approach to optimization of the model, which would include here real space refinement, automated fixing of rotamers, as well as peptide and NQH flips. The form of the model includes the actual structure, and variable parameters that describe it, which here include TLS modeling of ADPs. Additionally different restraints can be applied during the refinement, in this case NCS restraints on coordinates and/or B-factors.

Real space refinement: refinement of coordinate positions against the real space electron density maps.

Non-crystallographic symmetry (NCS) restraints: NCS refers to more than one copy of a molecule in the asymmetric unit of the crystal (i.e. the fundamental irreducible unit of the crystal). The global NCS restraint method used here involves a coordinate superposition of the related models followed by the calculation of the average model, and subsequent restraint of each model to that average. The superposition and averaging is repeated at each cycle of model optimization. The effect of these restraints is to make the copies of the molecules similar. This decreases the effective number of parameters refined and can improve model quality in some cases.

Fix rotamers: Protein side chains have sets of most common rotamers. This algorithm identifies side chains that are either rotamer outliers as defined by the Richardson rotamer library (Lovell et al., 2000) or are side chains with poor fit to the experimental electron density maps. For each side chain that is corrected, the method rotates each torsion angle moving out from the backbone looking for the best real-space fit to the density. The maps are not calculated after each rotamer correction, but instead are recalculated after all flagged rotamers have gone through the correction protocol once. Each correction is then validated against the recalculated maps, and those side-chains that are not an improvement over the original orientation are returned to the original orientation. This whole process is considered a macrocycle, and the user may specify the number of macrocycles for rotamer correction.

Flip peptides: Rotates the peptide backbone by 180 degrees to best fit the model to the electron density maps.

NQH flips: Asn, Gln, and His residues can often be fit favorably to the data in two orientations, related by a 180° rotation. In many cases, however, only one of these orientations is sterically and electrostatically favorable. *Phenix.refine* uses *Reduce* (Word et al., 1999) to identify Asn, Gln, and His residues that should be flipped, and then flips them automatically.

Translation, Libration (or rotation), Screw refinement (TLS): This is a method of refining the ADPs that considers the coordinated motion of groups of atoms, which thus uses less parameters that individual ADP refinement. The TLS formalism is a constrained anisotropic ADP refinement. TLS refers to three types of motion that can be

used to describe a displacement. A secondary structural element or an entire domain could define a group. For example, a protein can be partitioned into different numbers of groups. Both the borders for the groups and the number of groups can have a significant impact on the effectiveness of the TLS refinement. In this work we compared two approaches, *TLSMD*, and *phenix.find_tls_groups*. TLSMD allows the user to specify the number of TLS groups, from 1-20. The approach incorporated into PHENIX yields a single answer for partitioning the protein into TLS groupings.

Supplemental Data

Figure S1, related to Figure 1

(**A**) Plots of R_{free} with RMSD bonds or angles or R_{work}. For each structure the indicated results of the 256 ExCoRs are plotted. The red circles represent the 10% of the ExCoRs with the lowest R_{free} (e.g. 25/256). The dashed black lines represent the starting values for the PSI structures, or the values from the control refinement for the ER structures.

(**B**) Plots of R_{free} versus Mol Probity clash score. For each structure, the indicated results of the 256 ExCoRs are plotted. The dashed red lines represent starting values obtained from the deposited PSI model.

(**C**) Plots of R_{free} versus percent of residues with some weak density. For each structure, the indicated results of the 256 ExCoRs are plotted. The dashed red lines represent starting values obtained from the deposited PSI model.

(**D**) Automated vs manual rebuilding with ExCoR. We solved five different ligand-bound ER LBD structures using PHENIX AutoMR, followed by PHENIX Autobuild. The structures were then manually inspected and rebuilt in Coot, followed by ligand docking and ExCoR. These were compared with structures that went straight into ExCoR with only ligand docking, and no manual rebuilding. For each set of 256 ExCoRs, the R_{free} was plotted against the RMSD of bond lengths or angles.

(**E**) ExCoR error distribution and statistical analysis. Obtaining models with decreased R_{free} is not due to noise in the refinement procedure. The R_{free} from ExCoR refinement is shown as a frequency distribution, with black bars representing the bins. The green line indicates the starting R_{free} from the deposited pdb. The red line shows the frequency distribution of the noise for refinement of each structure, using the outlined procedure. Briefly, R_{free} was removed, and two new test sets were assigned. Both new data sets were subject to 256 ExCoR refinements, the difference between the resulting R_{free} was computed, and plotted here as the noise. The noise distribution was centered on the control refinement R_{free}. Note that the non-Guassian distribution of the data derives from the strong effects of NCS or TLS in some cases. These data demonstrate that ExCoR results can be distinguished from noise, as long as R_{free} improves by more than approximately 1% (e.g. 3OI7), which is largely the case.

(**F**) For the 35 PDB models (listed in table S1A) from PSI labs, the R_{free} range of ExCoR (signal) was compared to the R_{free} range obtained after control refinement of each structure using two new R_{free} sets (noise).

(**G**) Effect of changing R_{free} flags on the effectiveness of refinement strategies. R_{free} of models obtained from ExCoR of the indicated PDB structures using a set of R_{free} flags were plotted in decreasing order (black). R_{free} obtained from the same strategies using a different set of R_{free} flags are shown (red) for comparison.

(**H**) Correlation between R_{free} obtained from ExCoR using two different R_{free} flags. R_{free} obtained upon ExCoR of the indicated PDB structures using one set of R_{free} flags was

plotted against those obtained with the same strategies but using a different set of R_{free} flags. The correlation coefficient, R^2 is indicated.

(**I**) R_{sleep} versus R_{free} – For the indicated structures, the R_{free} reflections were removed completely from the data set and set aside as the R_{sleep} test set, and then a new R_{free} test set was selected and used for ExCoR. For each of the 256 new models obtained per structure, R_{sleep} was calculated using the removed R_{sleep} test set, and compared to the R_{free} obtained using the new test set.

(**J**) Effective strategies selected using a set of R_{free} flags are also effective using a different set of R_{free} flags. ExCoR strategies leading to the lowest R_{free} models were selected using a set of R_{free} flags #1, and compared to corresponding starting and control models using a different set of R_{free} flags #2.

A ER: Lowest Rfree ≈ lowest RMSD bonds or angles

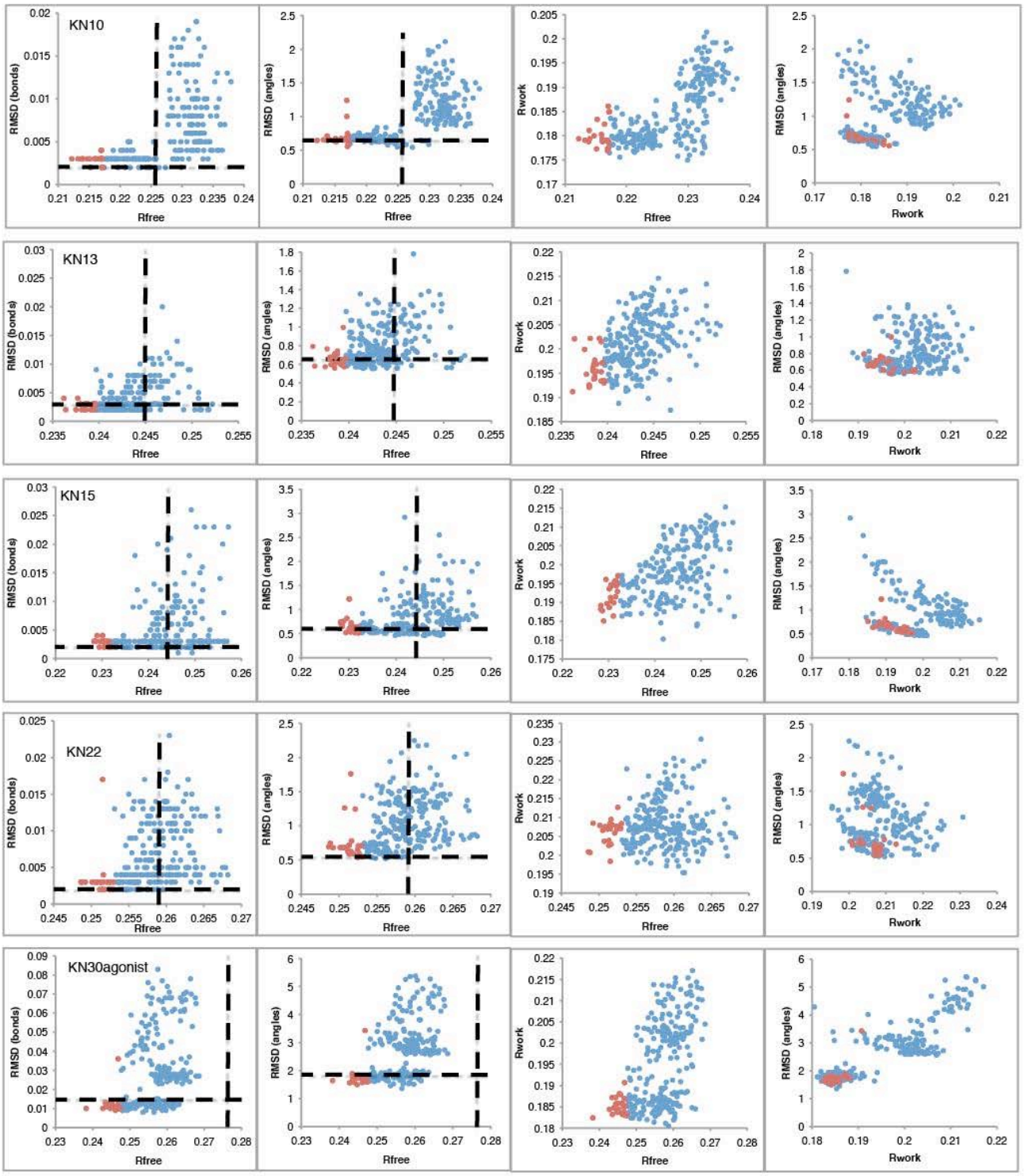

Fig. S1A-1

ER: Lowest Rfree ≈ lowest RMSD bonds or angles

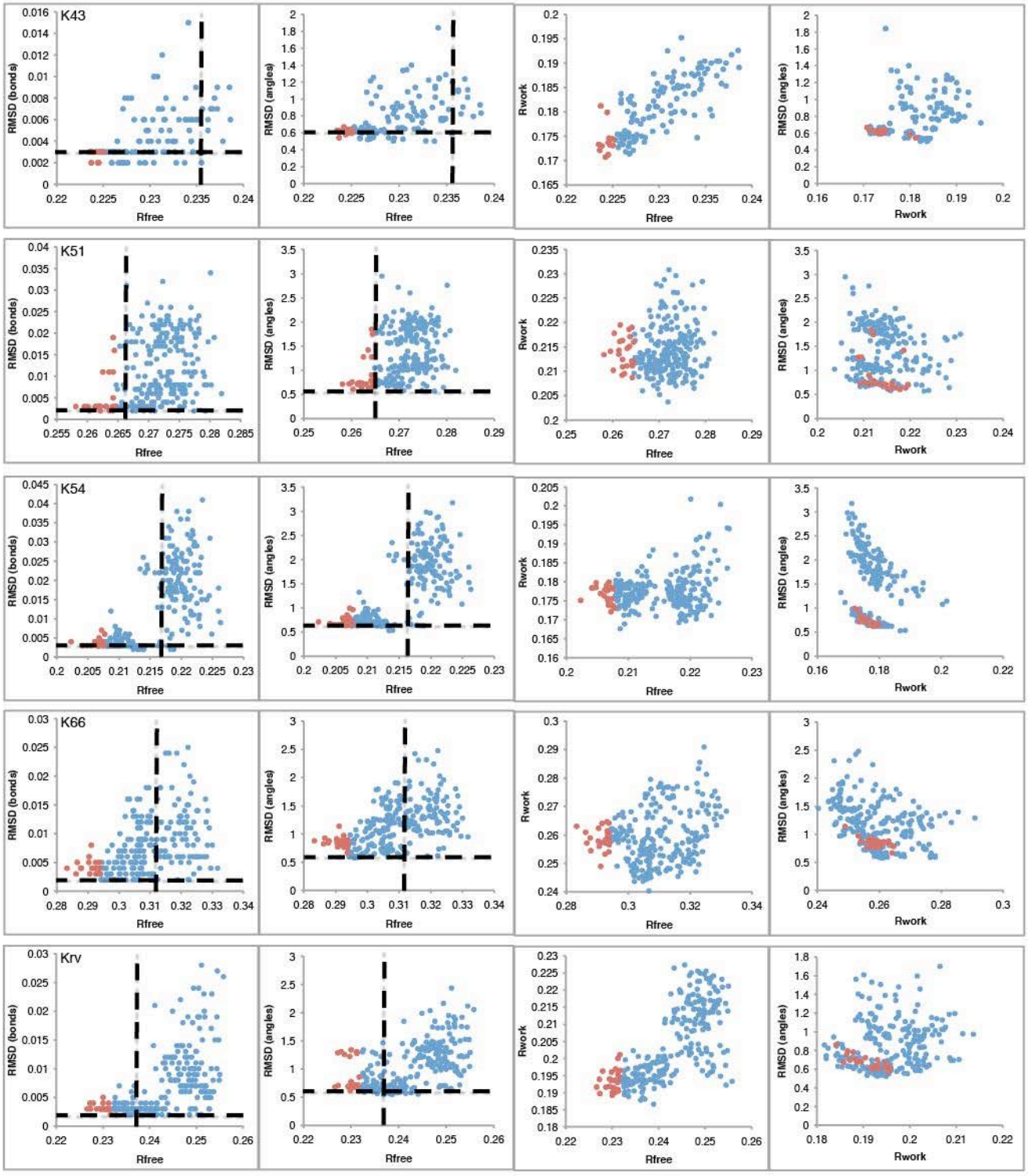

Fig. S1A-2

ER: Lowest Rfree ≠ lowest RMSD bonds or angles

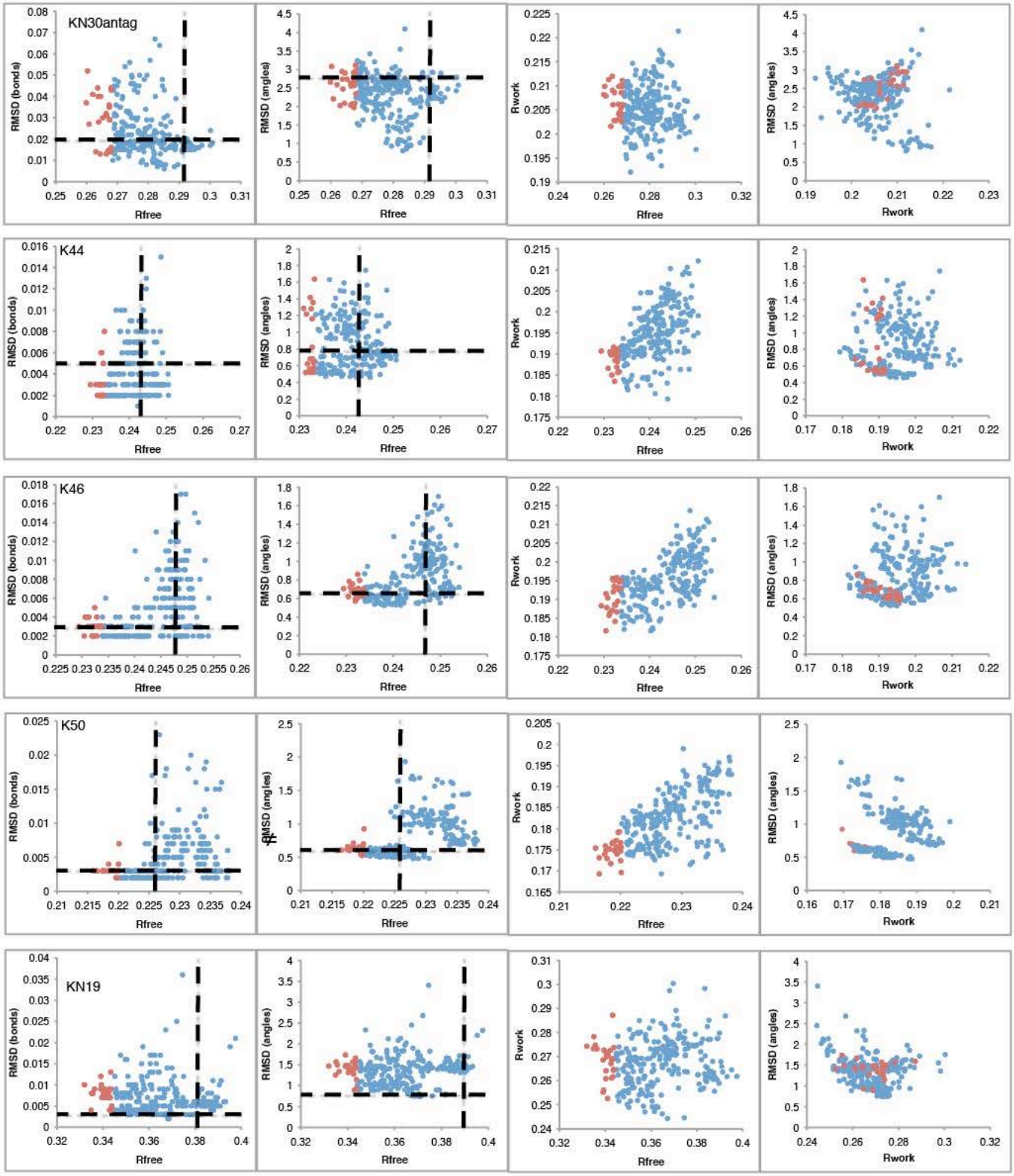

Fig. S1A-3

ER: Lowest Rfree ≠ lowest RMSD bonds or angles

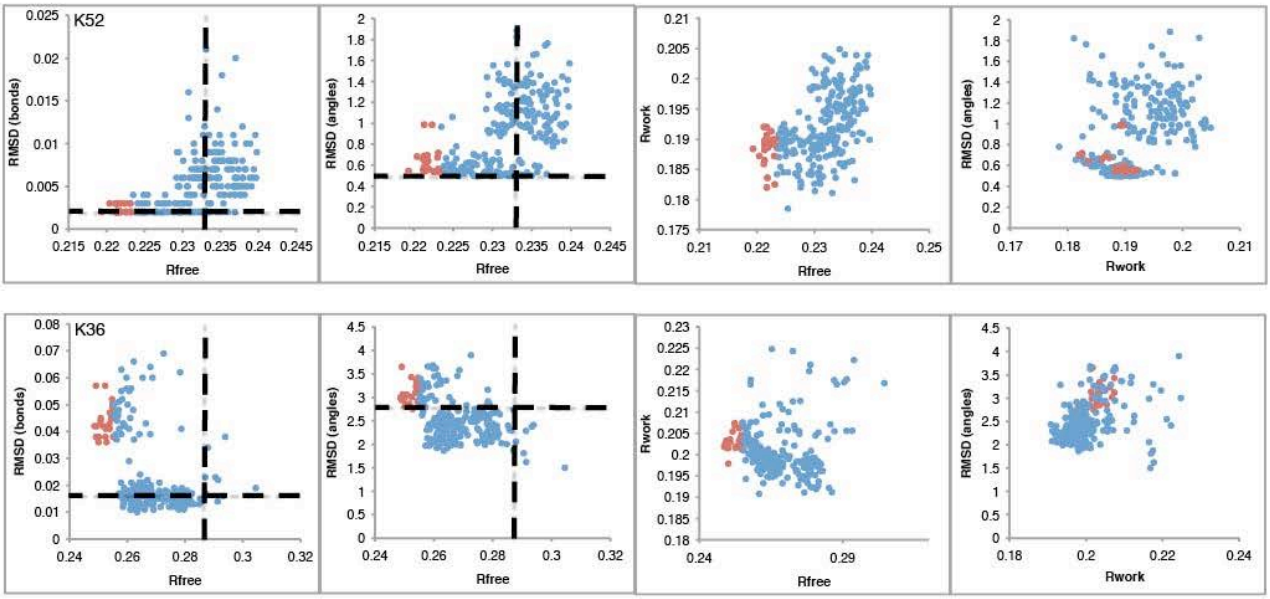

Fig. S1A-4

PSI: Lowest Rfree ≈ lowest RMSD bonds or angles

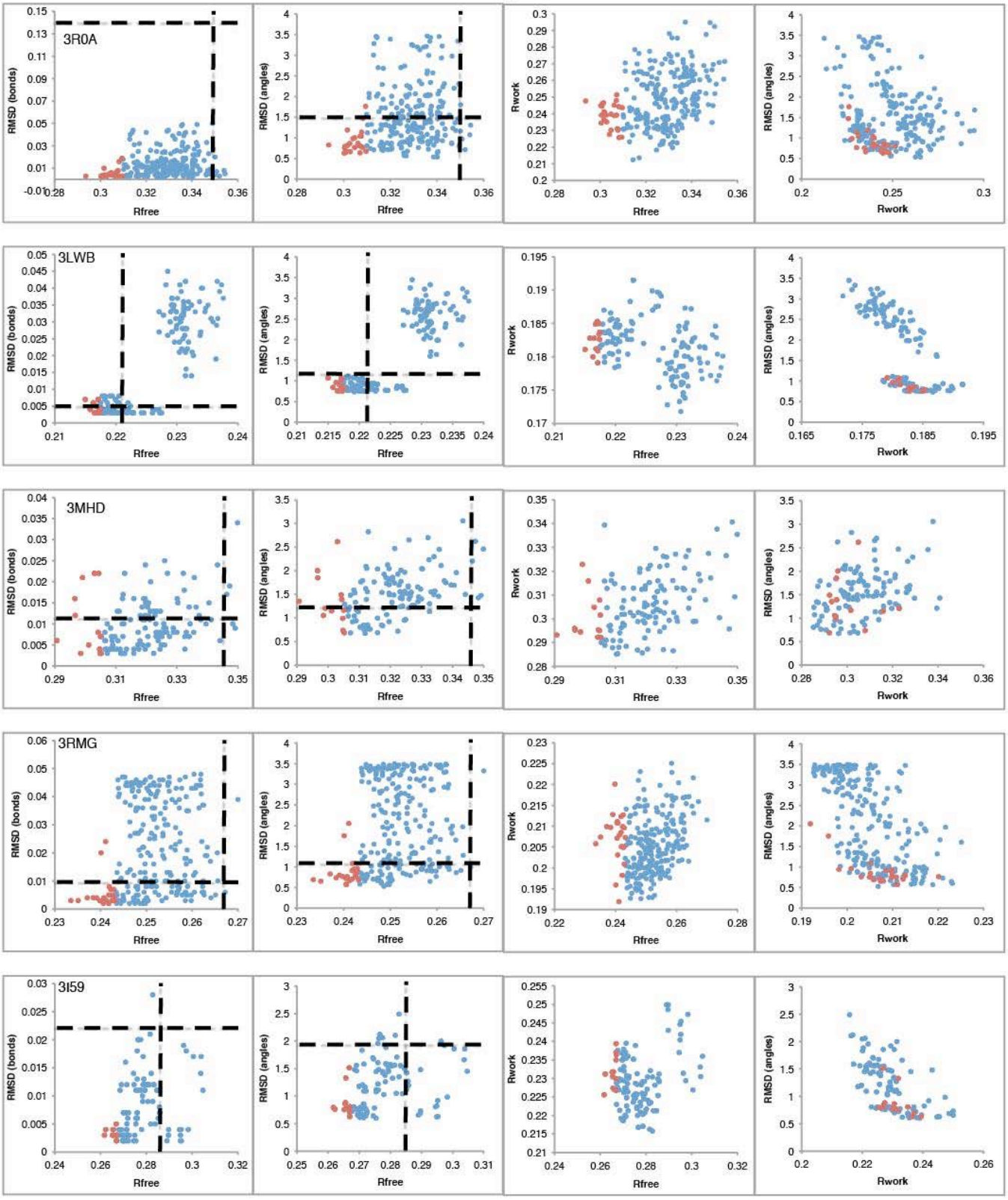

Fig. S1A-5

PSI: Lowest Rfree ≈ lowest RMSD bonds or angles

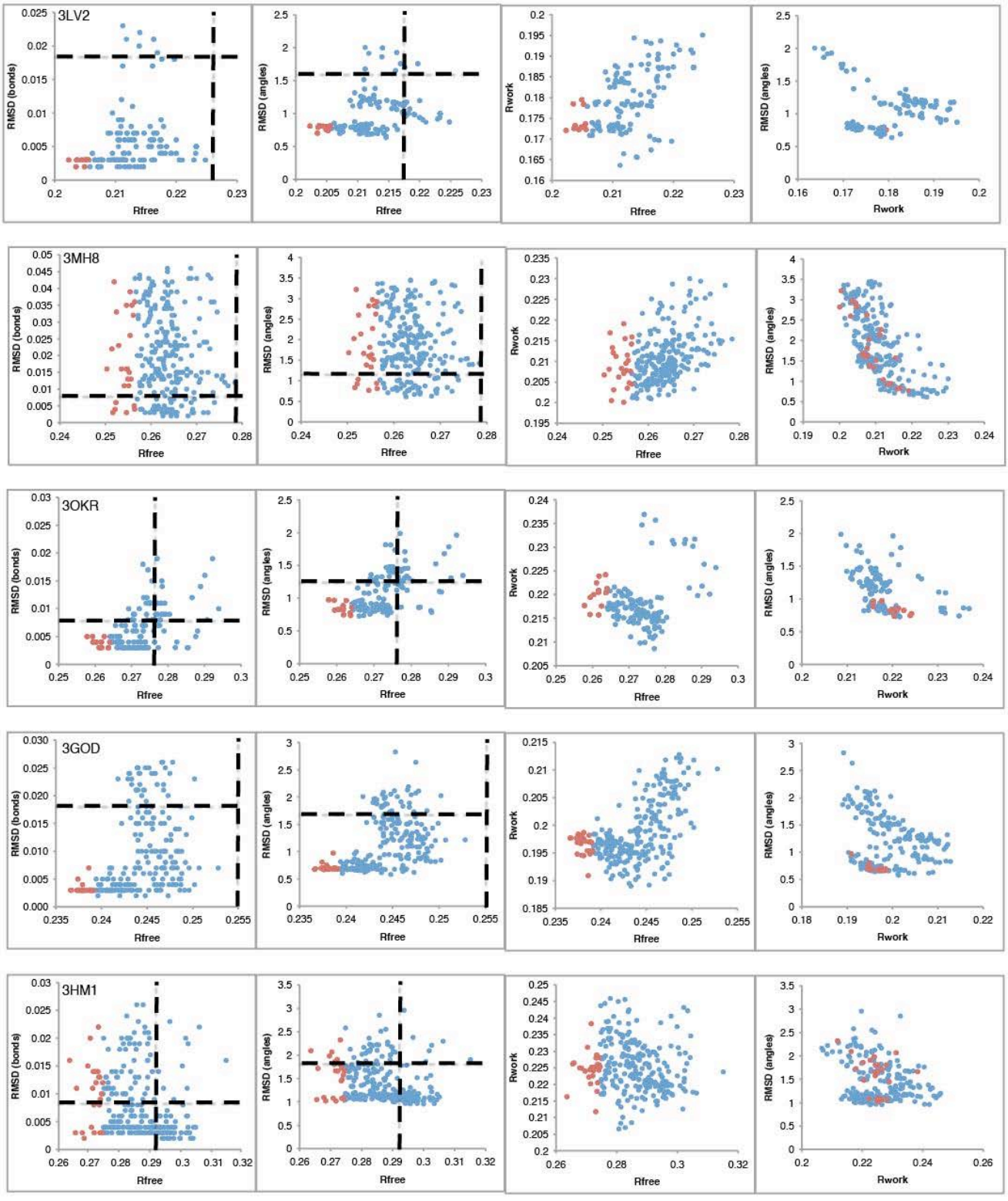

Fig. S1A-6

PSI: Lowest Rfree ≈ lowest RMSD bonds or angles

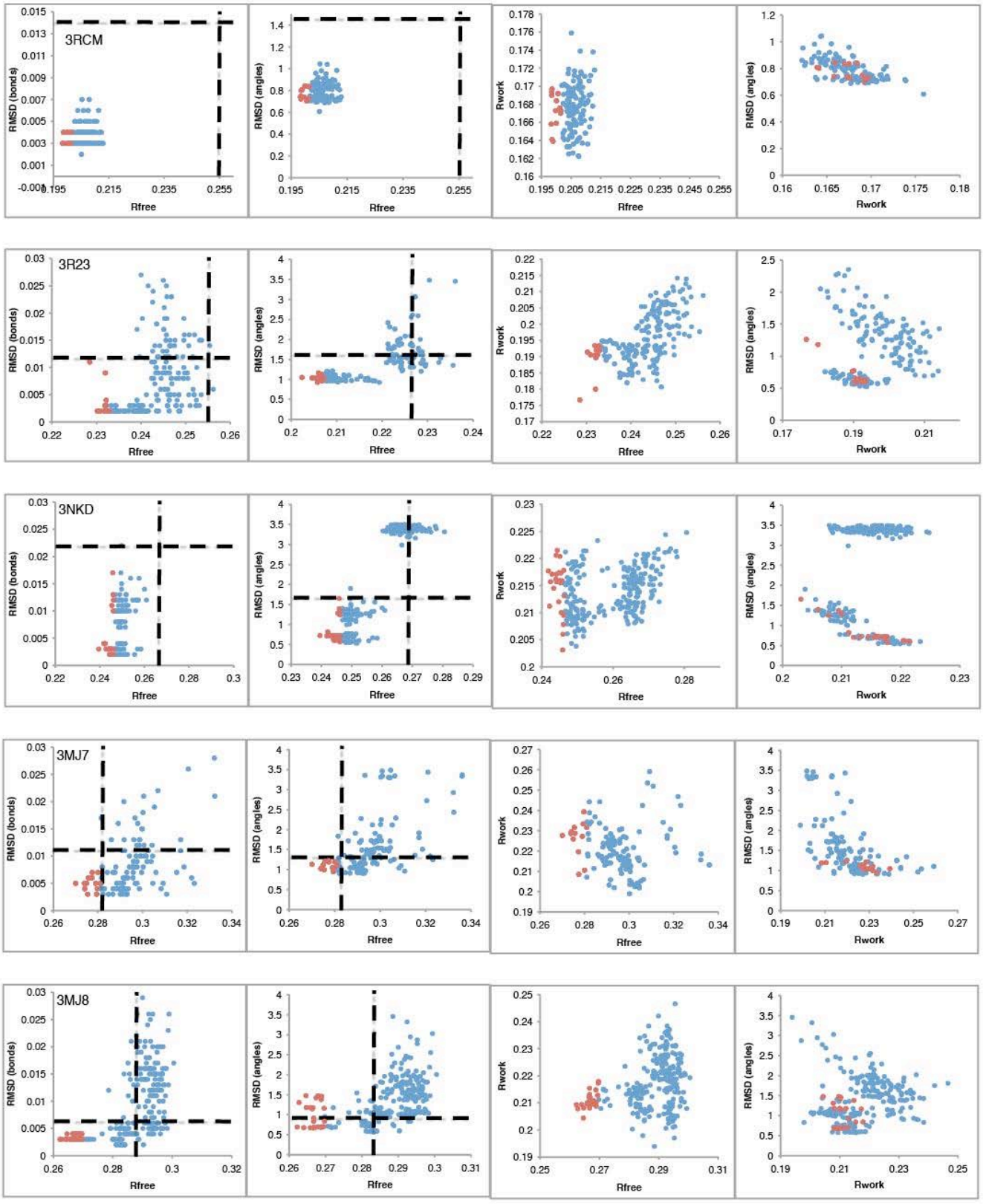

Fig. S1A-7

PSI: Lowest Rfree ≈ lowest RMSD bonds or angles

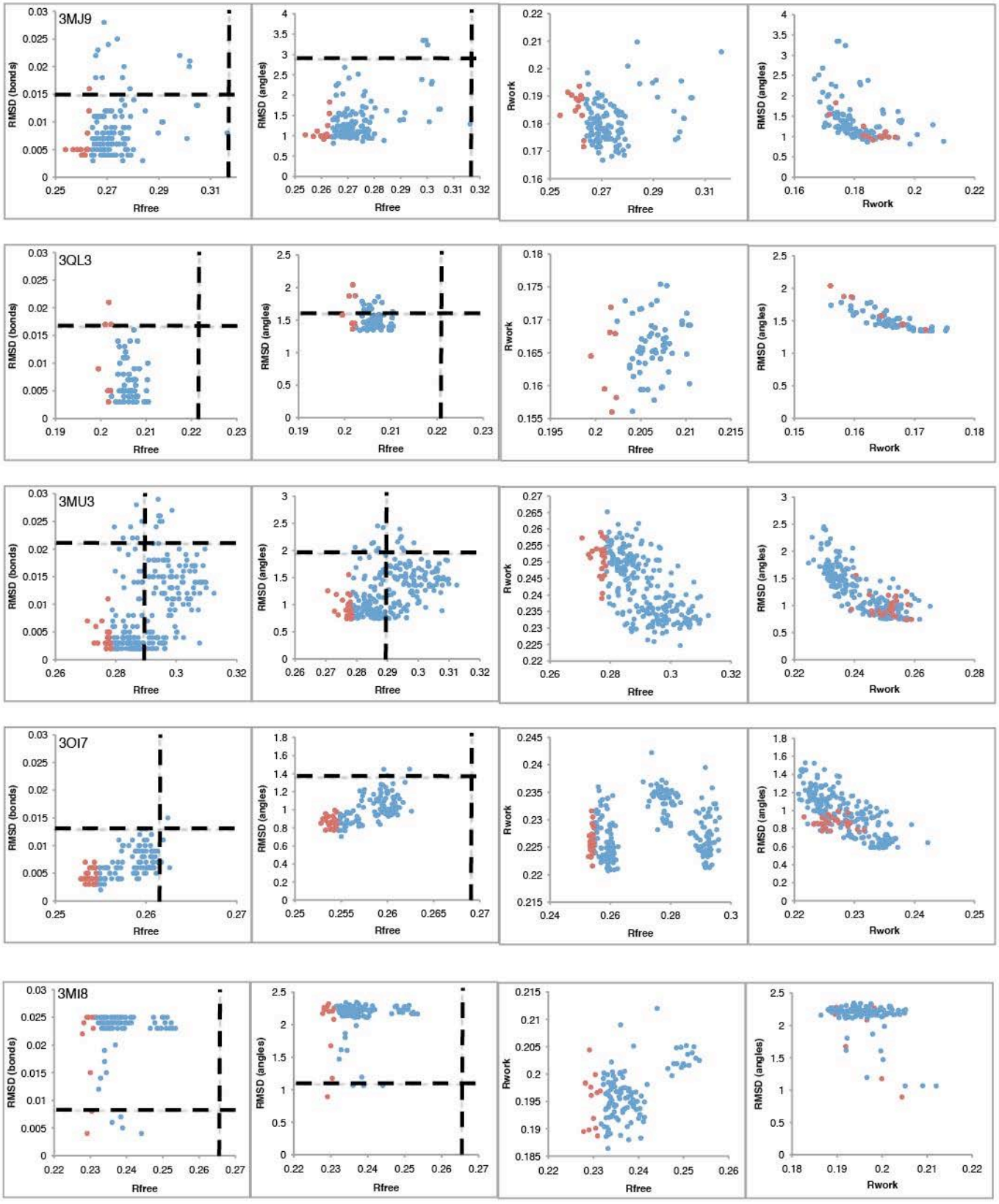

Fig. S1A-8

PSI: Lowest Rfree ≠ lowest RMSD bonds or angles

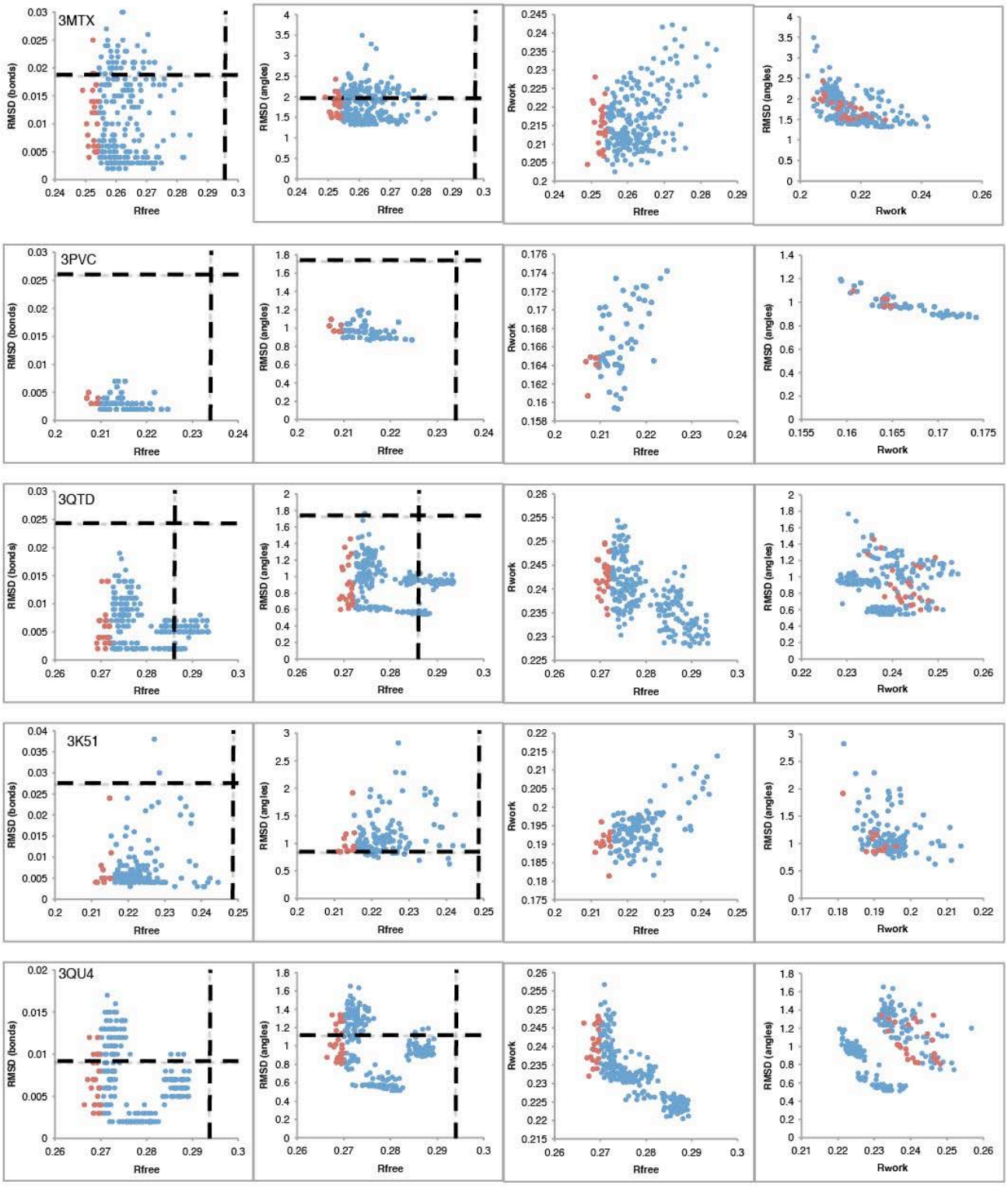

Fig. S1A-9

PSI: Lowest Rfree ≠ lowest RMSD bonds or angles

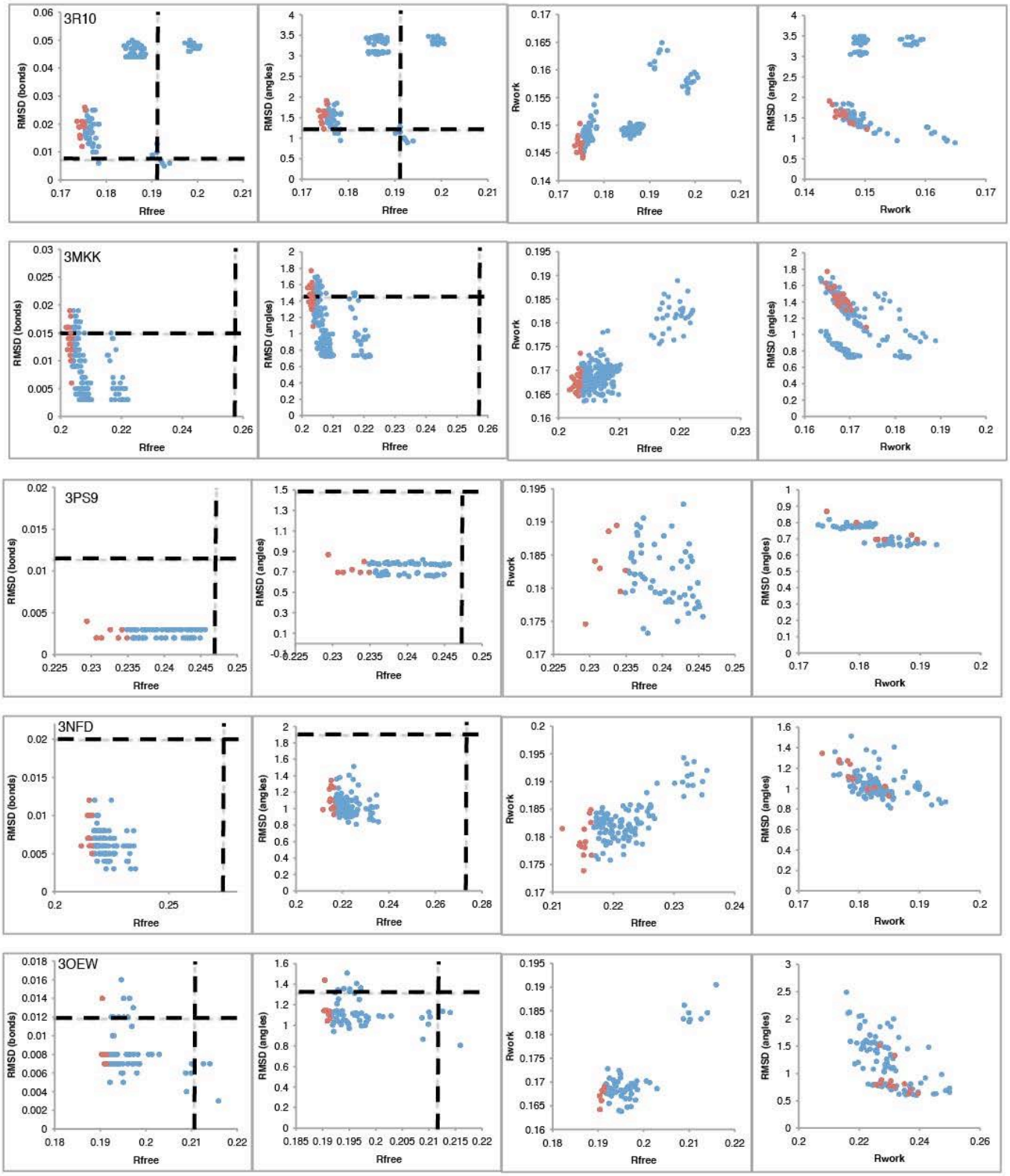

Fig. S1A-10

PSI: Lowest Rfree ≠ lowest RMSD bonds or angles

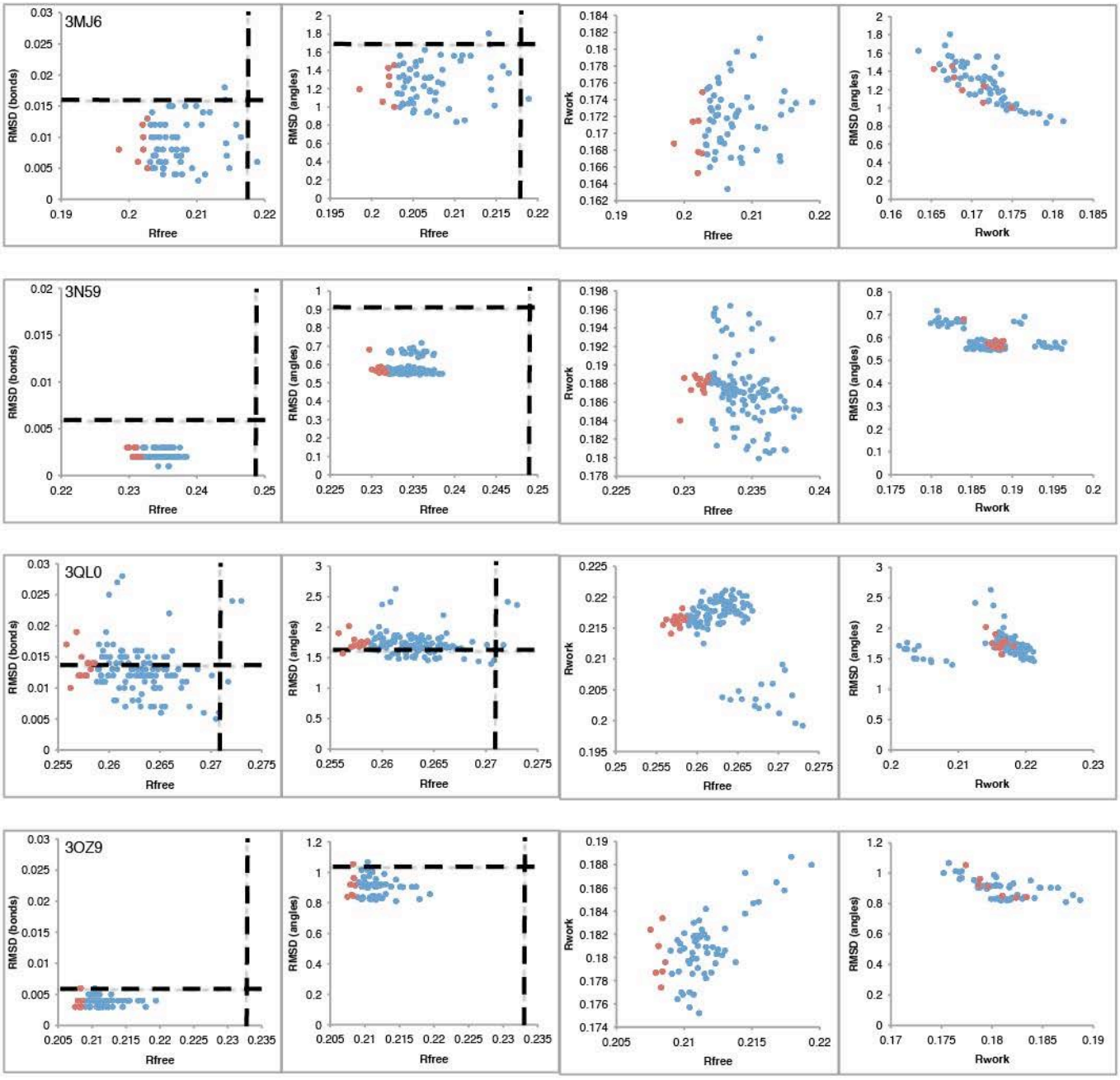

Fig. S1A-11

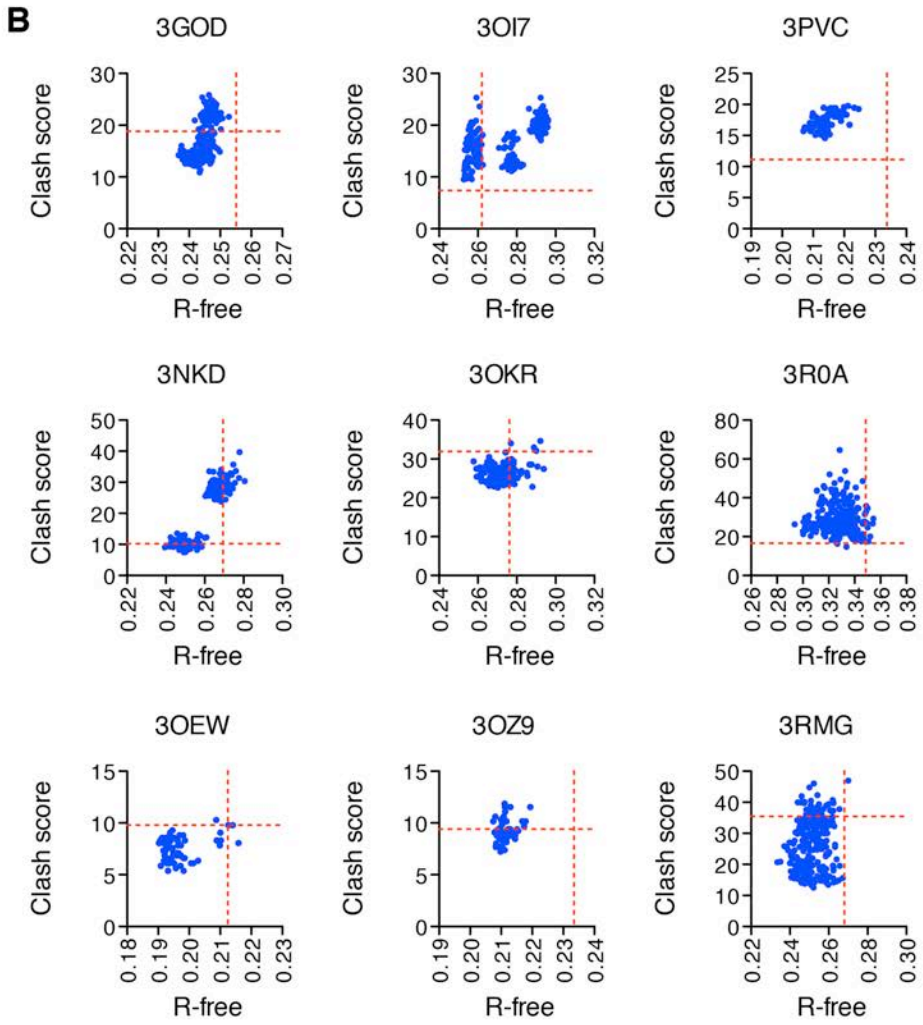
B
3GOD
3OI7
3PVC
3NKD
3OKR
3R0A
3OEW
3OZ9
3RMG
Clash score
R-free

Fig. S1B

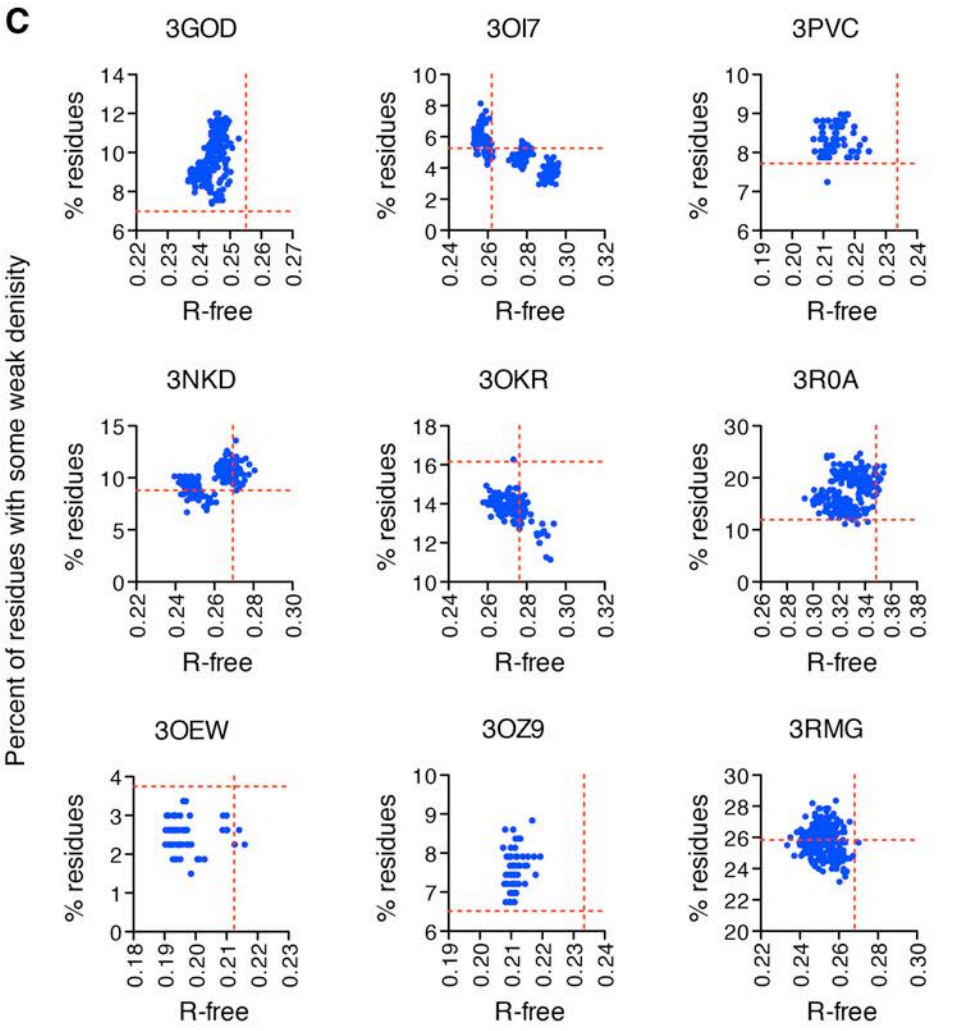
C
Percent of residues with some weak denisity
3GOD
3OI7
3PVC
3NKD
3OKR
3R0A
3OEW
3OZ9
3RMG
% residues
R-free

Fig. S1C

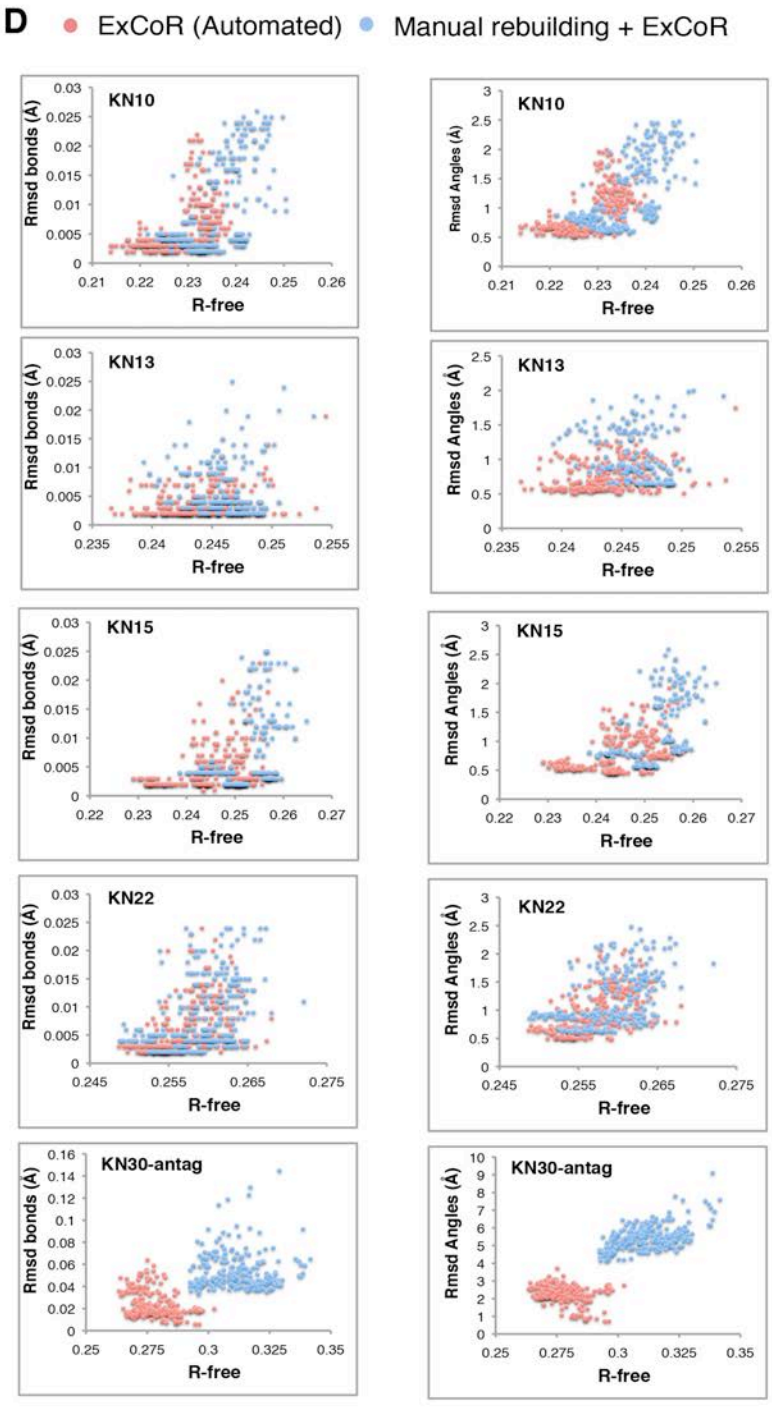
D
ExCoR (Automated)
Manual rebuilding + ExCoR
KN10
Rmsd bonds (Å)
Rmsd Angles (Å)
R-free
KN13
KN15
KN22
KN30-antag

Fig. S1D

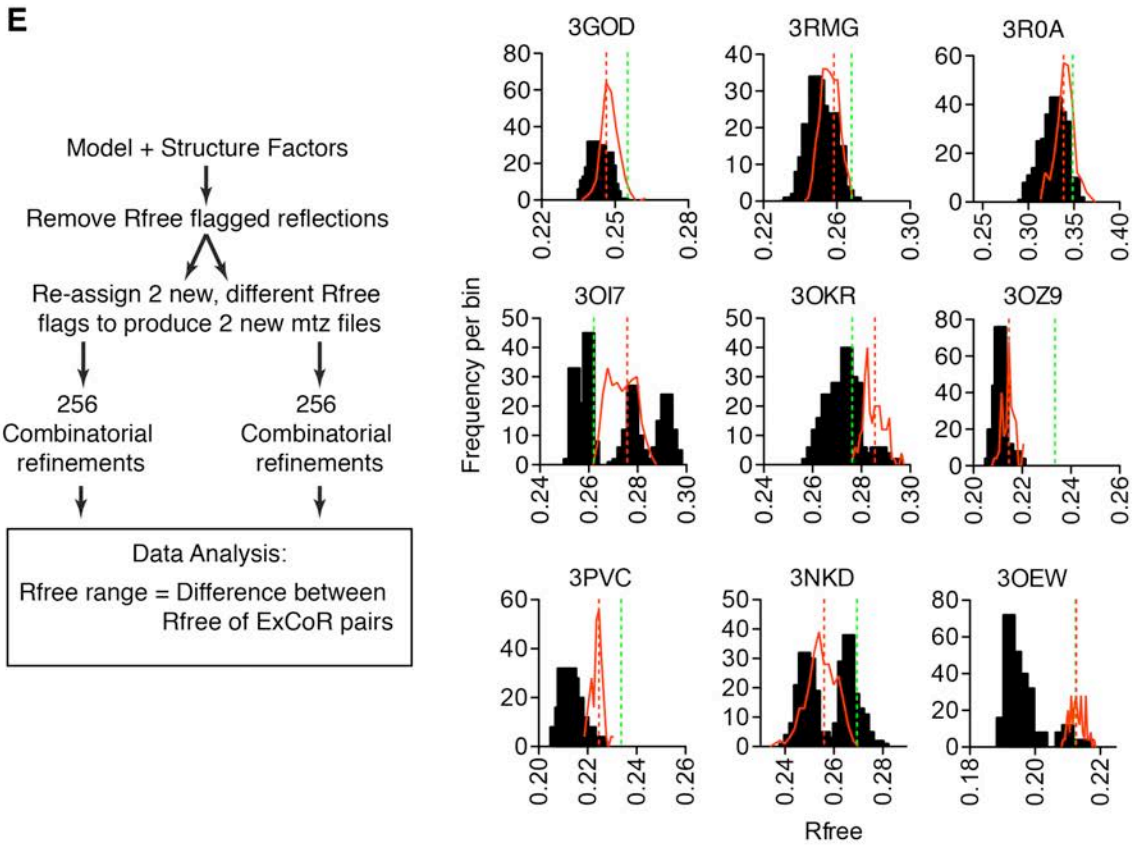
E
Model + Structure Factors
Remove Rfree flagged reflections
Re-assign 2 new, different Rfree flags to produce 2 new mtz files
256 Combinatorial refinements
256 Combinatorial refinements
Data Analysis:
Rfree range = Difference between Rfree of ExCoR pairs
3GOD
3RMG
3R0A
3OI7
3OKR
3OZ9
3PVC
3NKD
3OEW
Frequency per bin
Rfree

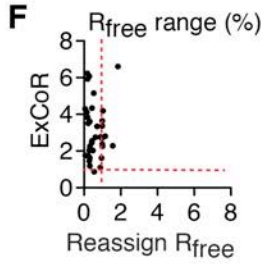
F
Rfree range (%)
ExCoR
Reassign Rfree

Fig. S1E-F

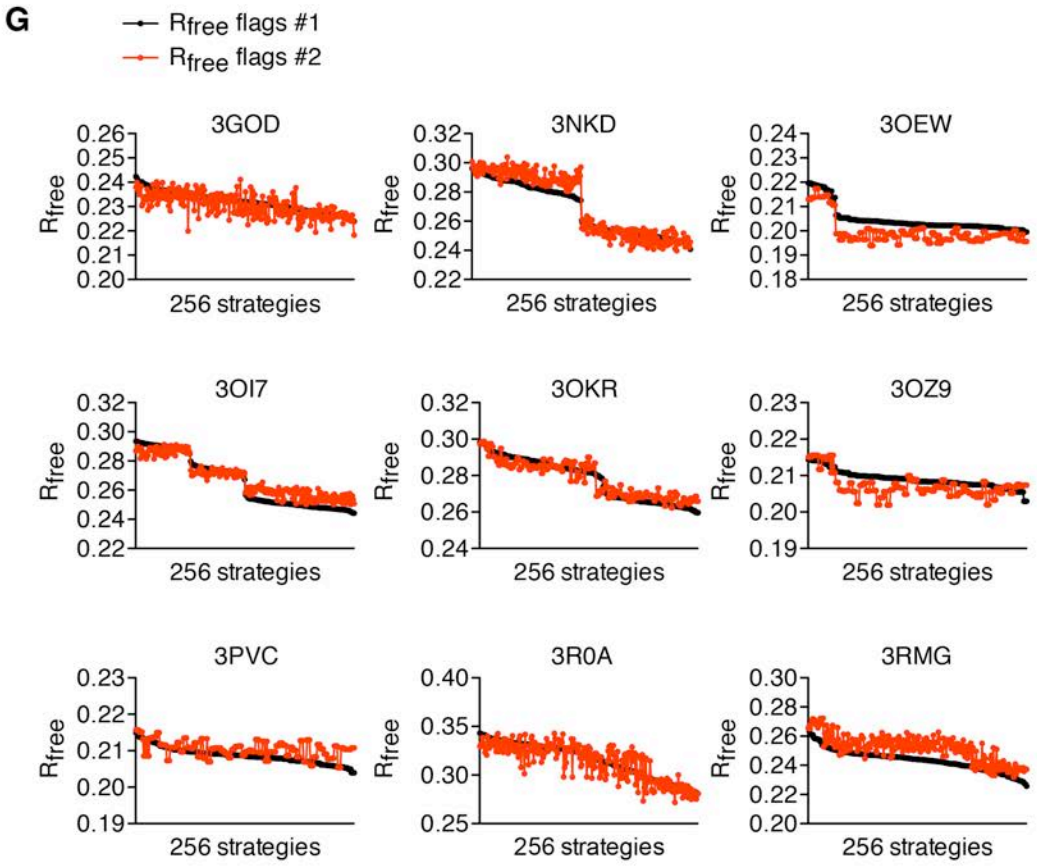
G
Rfree flags #1
Rfree flags #2
3GOD
3NKD
3OEW
3OI7
3OKR
3OZ9
3PVC
3R0A
3RMG
Rfree
256 strategies

Fig. S1G

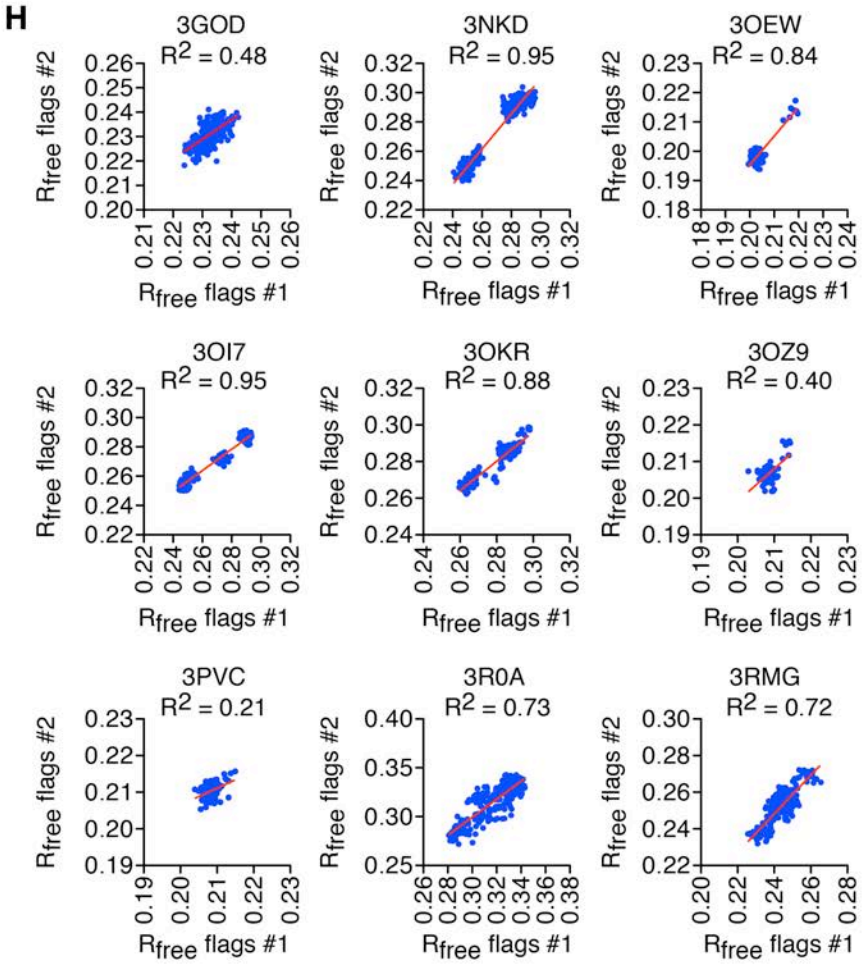
H
3GOD
R2 = 0.48
3NKD
R2 = 0.95
3OEW
R2 = 0.84
3OI7
R2 = 0.95
3OKR
R2 = 0.88
3OZ9
R2 = 0.40
3PVC
R2 = 0.21
3R0A
R2 = 0.73
3RMG
R2 = 0.72
Rfree flags #2
Rfree flags #1

Fig. S1H

I

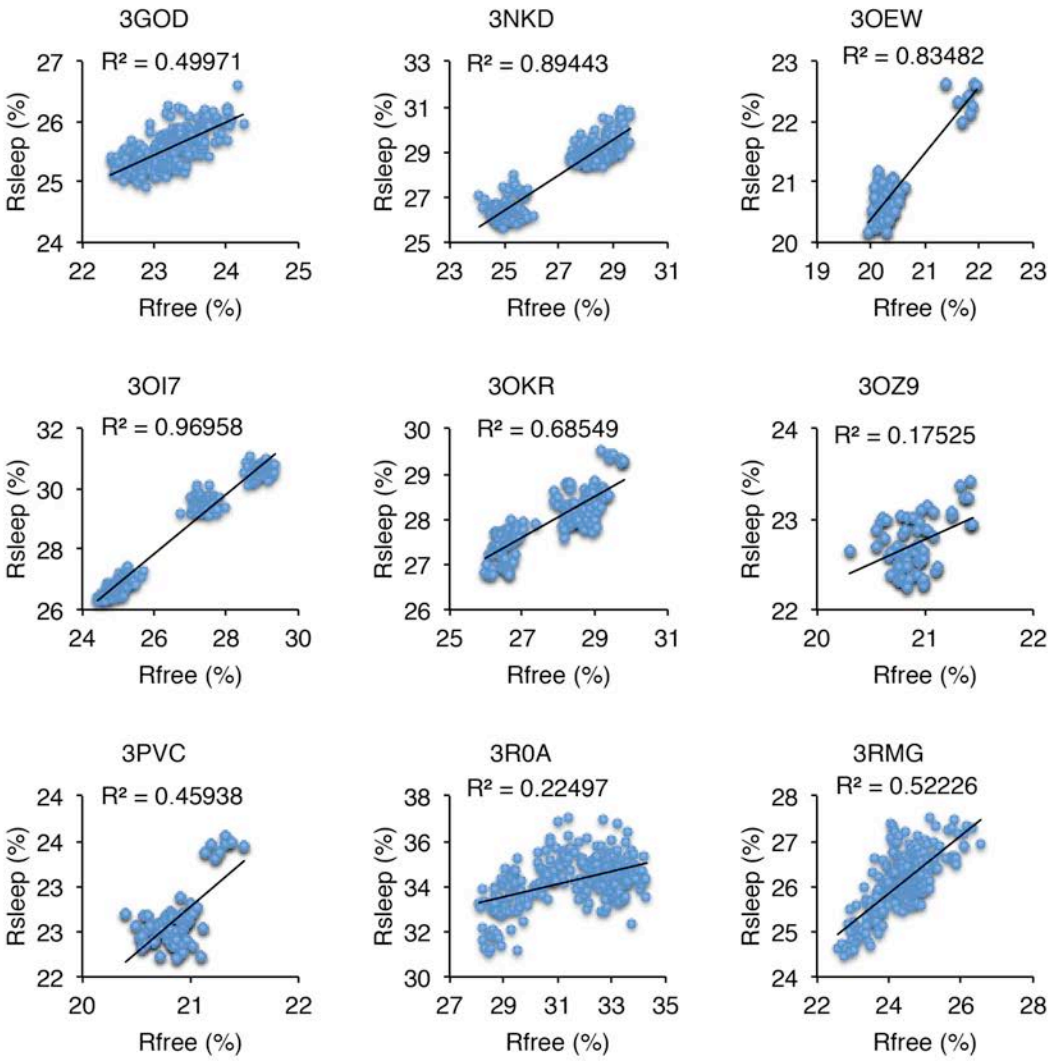
3GOD
R² = 0.49971
Rsleep (%)
Rfree (%)
3NKD
R² = 0.89443
Rsleep (%)
Rfree (%)
3OEW
R² = 0.83482
Rsleep (%)
Rfree (%)
3OI7
R² = 0.96958
Rsleep (%)
Rfree (%)
3OKR
R² = 0.68549
Rsleep (%)
Rfree (%)
3OZ9
R² = 0.17525
Rsleep (%)
Rfree (%)
3PVC
R² = 0.45938
Rsleep (%)
Rfree (%)
3R0A
R² = 0.22497
Rsleep (%)
Rfree (%)
3RMG
R² = 0.52226
Rsleep (%)
Rfree (%)

Fig. S1I

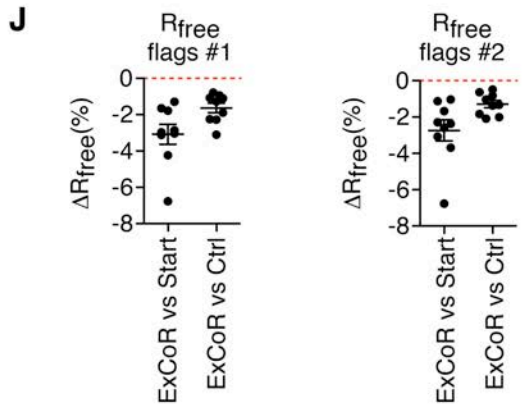
J
Rfree
flags #1
ΔRfree(%)
0
-2
-4
-6
-8
ExCoR vs Start
ExCoR vs Ctrl
Rfree
flags #2
ΔRfree(%)
0
-2
-4
-6
-8
ExCoR vs Start
ExCoR vs Ctrl

Fig. S1J

Figure S2, related to Figure 2

Structural diversity, error correction and improved maps and ligand fitting obtained from ExCoR

(**A**) Error correction without map improvement. For these examples the error was automatically corrected for a subset of the ExCoR produced models. Ser213 side-chain in PDB 3MH8 is misplaced into the mainchain density, and the backbone carbonyl is also misplaced. Thirty-two different ExCoR-derived conformers from a single TLS grouping were examined, and the number of structures in that group is listed above each panel in parentheses. Only 2/32 ExCoR models corrected both errors. Asn90 from 3MH8 was misplaced and fixed by ExCoR. Thr128 and Val in 3MJ9 were misplaced and fixed by a subset of ExCoR models.

(**B**) Error correction with map improvement. Here ExCoR improved the maps and identified the correct conformers.

(**C**) Main-chain remodeling with improved maps.

(D-F) Improved ligand placement with ExCoR (**D**) Shown is the coenzyme A (PDB ID: 3NFD). The five membered ribose ring at the core of the ligand was misplaced into a water molecule in the deposited structure. Automated correction of the ribose placement with ExCoR allowed correcting shifts in the adenosine and phosphates. (**E**) Shown is a tamoxifen derivative (compound KN16) bound to ERα LBD, where only a subset of the models were correct for the hydrogen bonding, and a different set were correct for placement of the naphthalene group. (**F**) This ER ligand shows different ring conformers, which in turn alter the positioning of an adjacent hydroxyl group, and whether it forms the correct hydrogen bond.

(**G**) Identification of hidden alternate conformers from improved maps.

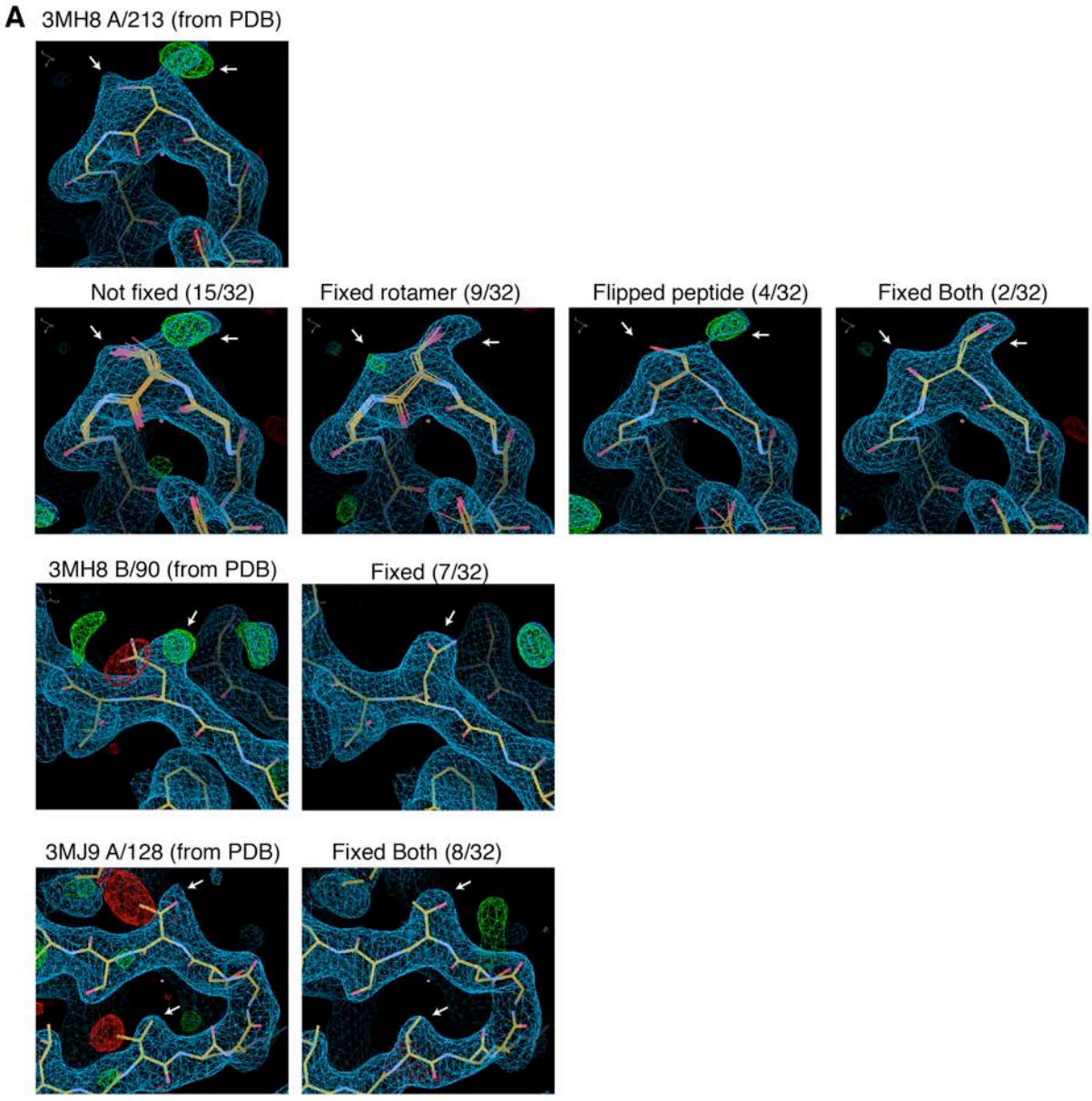
A
3MH8 A/213 (from PDB)
Not fixed (15/32)
Fixed rotamer (9/32)
Flipped peptide (4/32)
Fixed Both (2/32)
3MH8 B/90 (from PDB)
Fixed (7/32)
3MJ9 A/128 (from PDB)
Fixed Both (8/32)

Fig. S2A

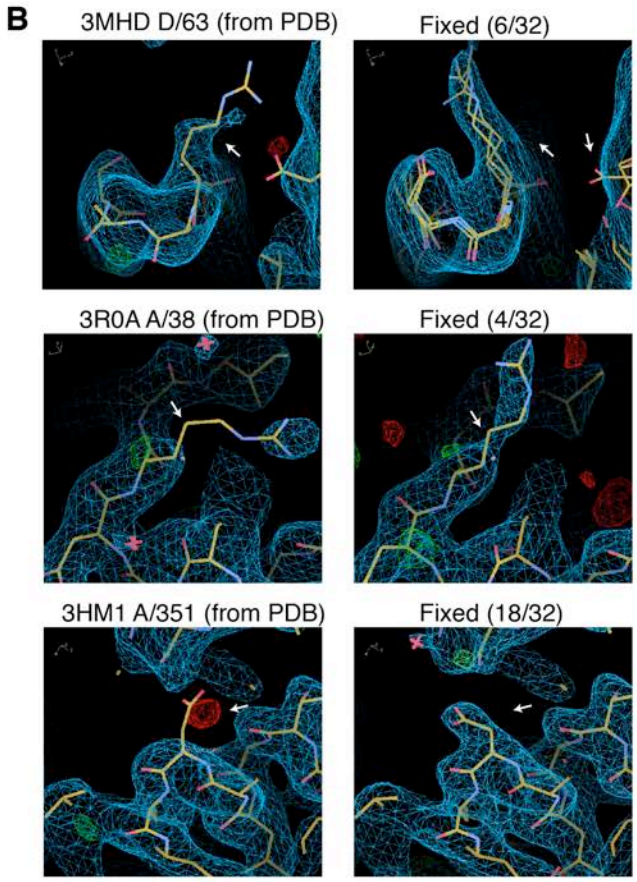
B
3MHD D/63 (from PDB)
Fixed (6/32)
3R0A A/38 (from PDB)
Fixed (4/32)
3HM1 A/351 (from PDB)
Fixed (18/32)

Fig. S2B

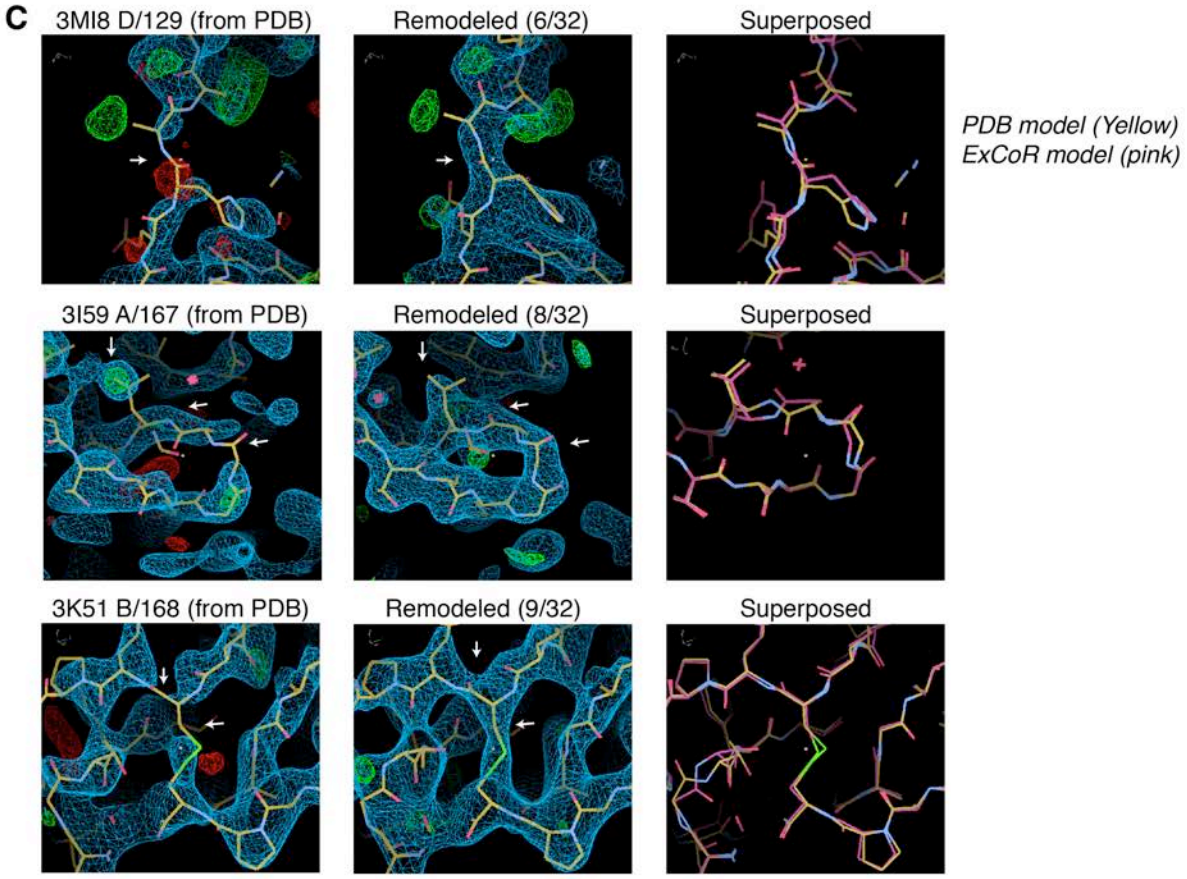
C
3MI8 D/129 (from PDB)
Remodeled (6/32)
Superposed
3I59 A/167 (from PDB)
Remodeled (8/32)
Superposed
3K51 B/168 (from PDB)
Remodeled (9/32)
Superposed
PDB model (Yellow)
ExCoR model (pink)

Fig. S2C

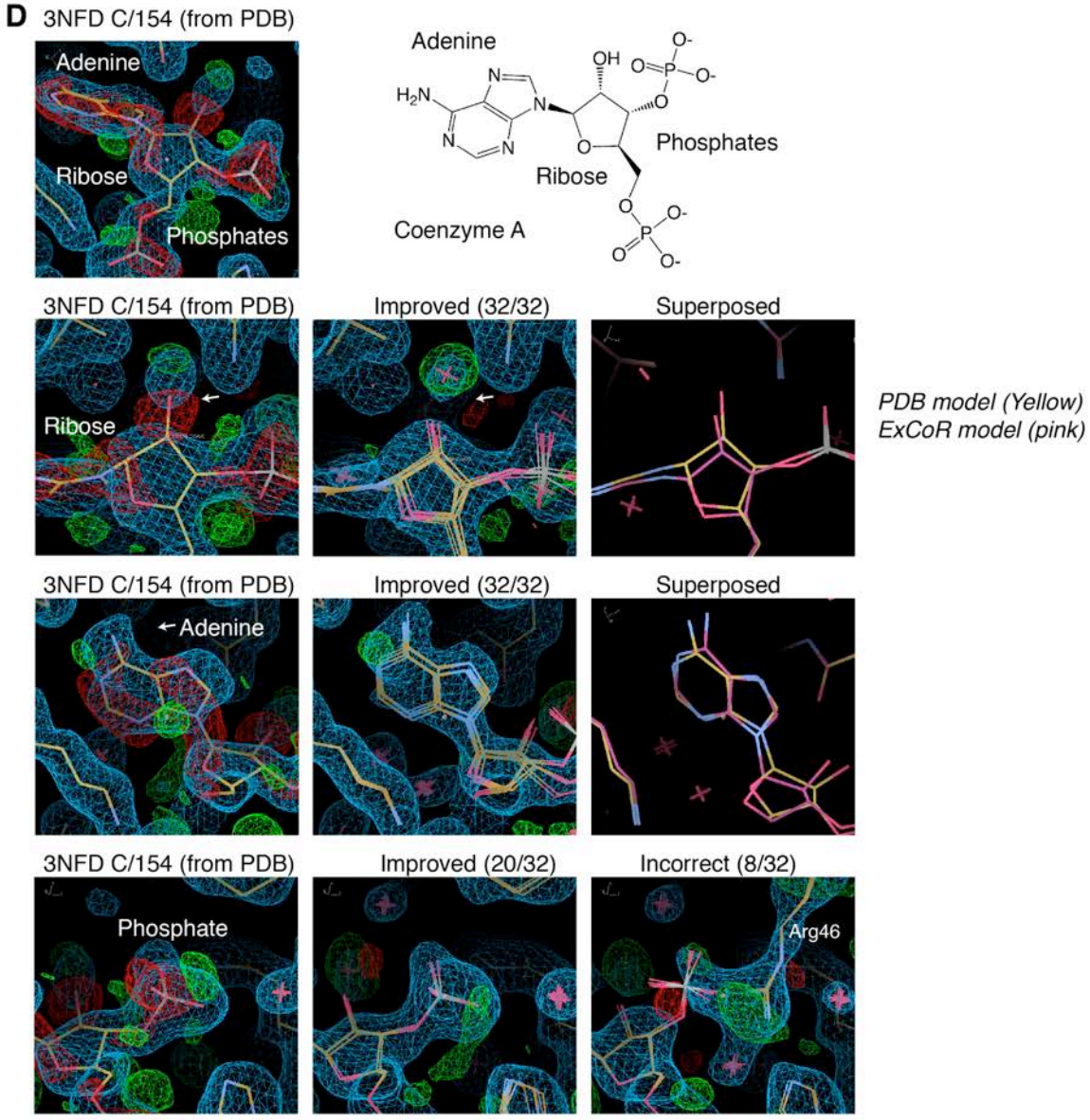
D
3NFD C/154 (from PDB)
Adenine
Ribose
Phosphates
Adenine
Phosphates
Ribose
Coenzyme A
3NFD C/154 (from PDB)
Improved (32/32)
Superposed
Ribose
PDB model (Yellow)
ExCoR model (pink)
3NFD C/154 (from PDB)
Improved (32/32)
Superposed
←Adenine
3NFD C/154 (from PDB)
Improved (20/32)
Incorrect (8/32)
Phosphate
Arg46

Fig. S2D

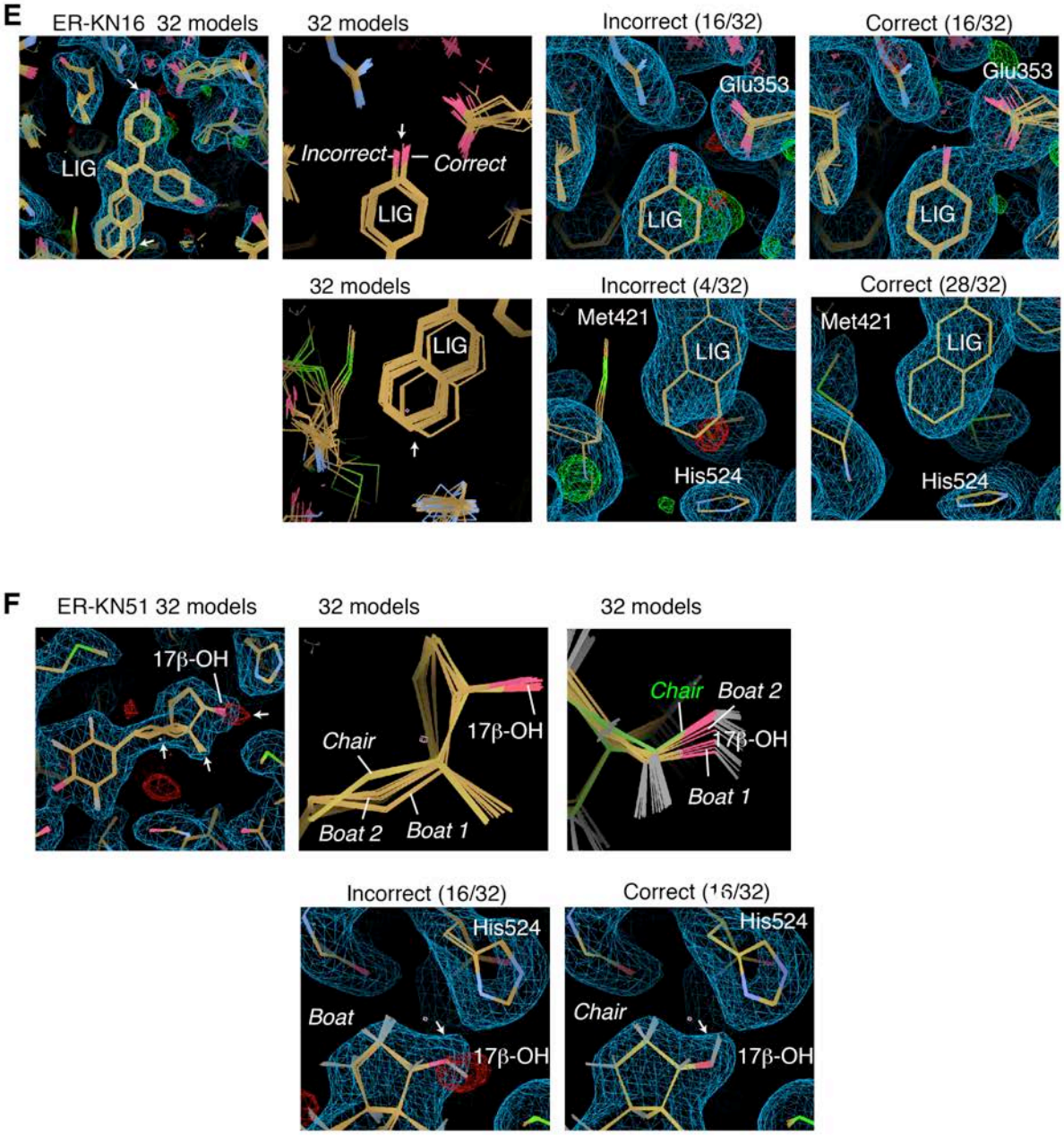
E
ER-KN16 32 models
LIG
32 models
Incorrect
Correct
LIG
Incorrect (16/32)
Glu353
LIG
Correct (16/32)
Glu353
LIG
32 models
LIG
Incorrect (4/32)
Met421
LIG
His524
Correct (28/32)
Met421
LIG
His524
F
ER-KN51 32 models
17β-OH
32 models
Chair
17β-OH
Boat 2
Boat 1
32 models
Chair
Boat 2
17β-OH
Boat 1
Incorrect (16/32)
His524
Boat
17β-OH
Correct (16/32)
His524
Chair
17β-OH

Fig. S2E-F

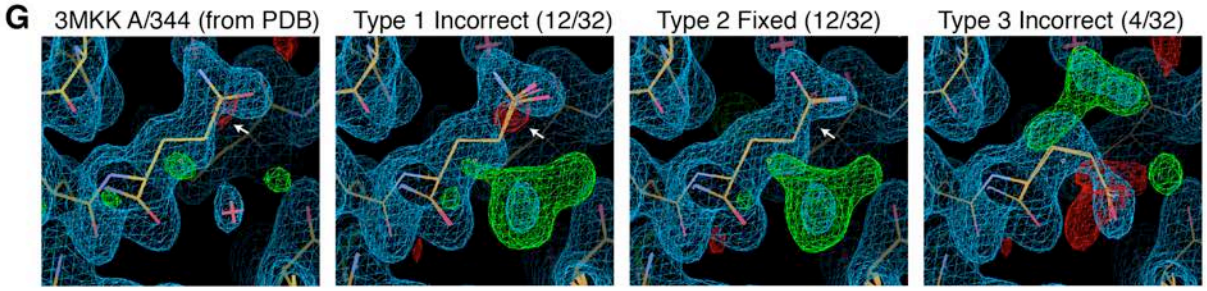

None of the 256 correctly adopted the type 3 conformer, because there are 2 alternate conformers suggested by the electron density within the type 3 models.

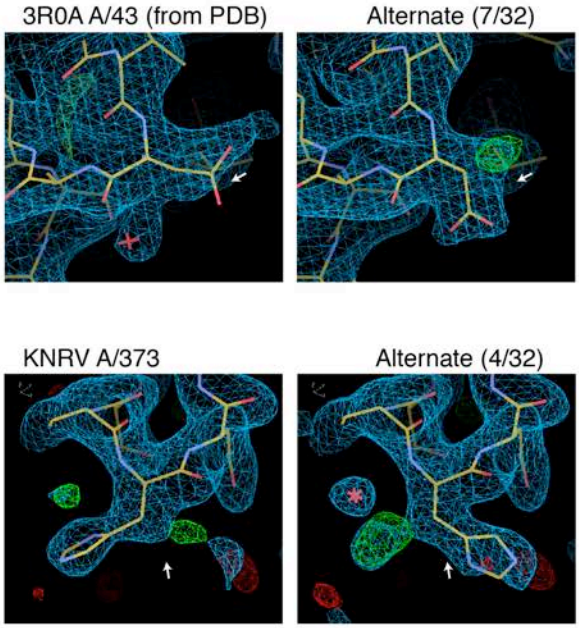

Fig. S2G

Figure S3, related to Figure 3

ExCoR of protein structures

35 recently deposited structures from 4 different PSI centers/labs were refined with ExCoR. 18 new ERα ligand-binding domain models refined using ExCoR after molecular replacement and automated rebuilding using PHENIX AutoMR and AUTOBUILD, respectively are also shown. The X-axis contains the 32 permutations of C = NCS, R = rotamer search, P = peptide flip, N = NQH flip, and S = real space refinement. Each line represents the refinements with the specified number of TLS groups /protein chain. The black line (TLS0) represents the refinements without TLS, with the control refinement (individual XYZ and ADP) being the point on the farthest left. The TLS groupings were defined with the TLSMD server or TLS grouping program of PHENIX (TLSph). Note that the use of NCS restraints in the case of the two KN30-bound ERα structures dictated blocks of best and worst outcomes, and this NCS "block effect" occurred frequently. Also note for structure 3MHD, that the Rotamers+Peptide flip led to a profound >4% improvement in R_{free} when the number of TLS groups was reduced from 15 to 9.

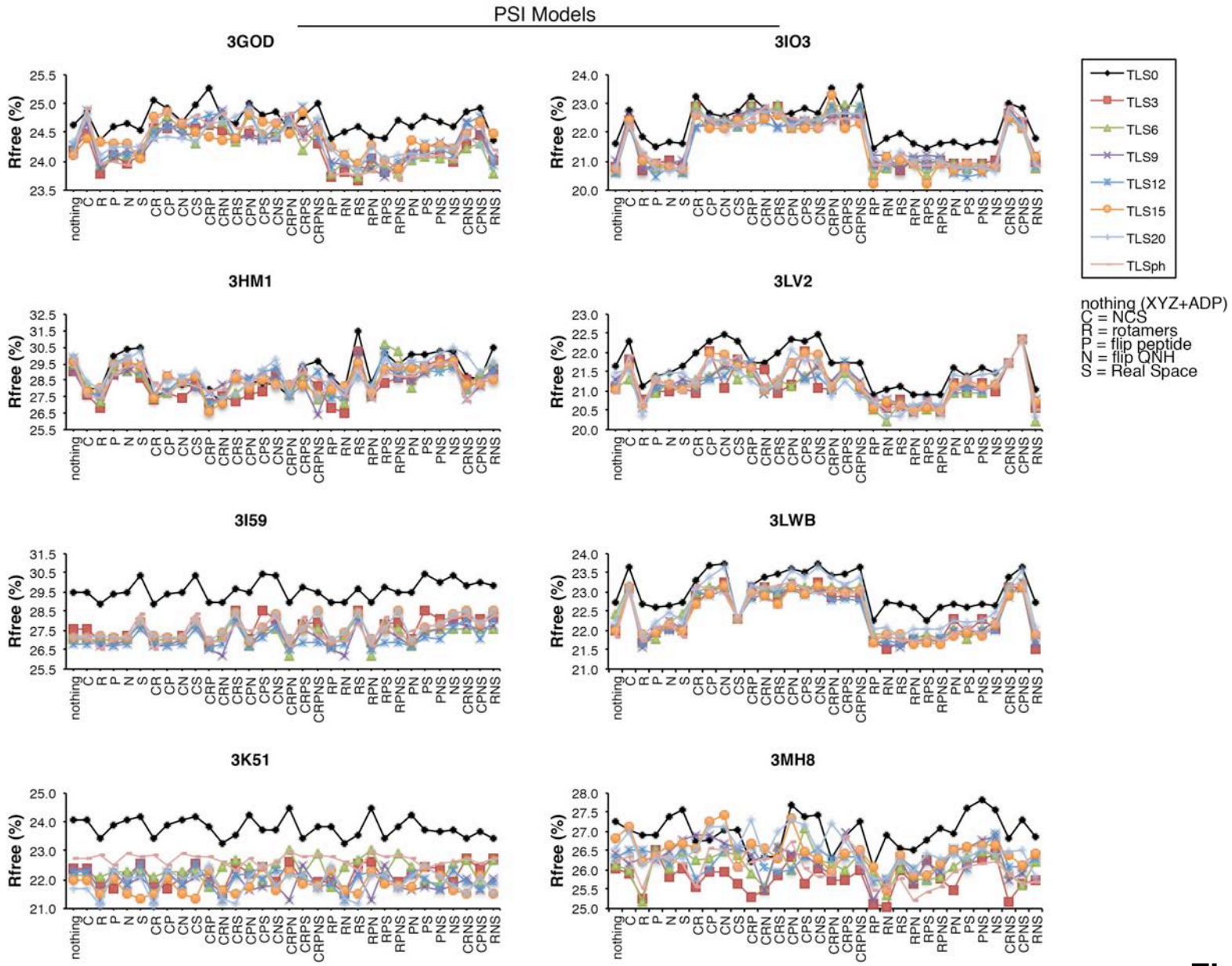
PSI Models
3GOD
3IO3
3HM1
3LV2
3I59
3LWB
3K51
3MH8
Rfree (%)
TLS0
TLS3
TLS6
TLS9
TLS12
TLS15
TLS20
TLSph
nothing (XYZ+ADP)
C = NCS
R = rotamers
P = flip peptide
N = flip QNH
S = Real Space

Fig. S3-1

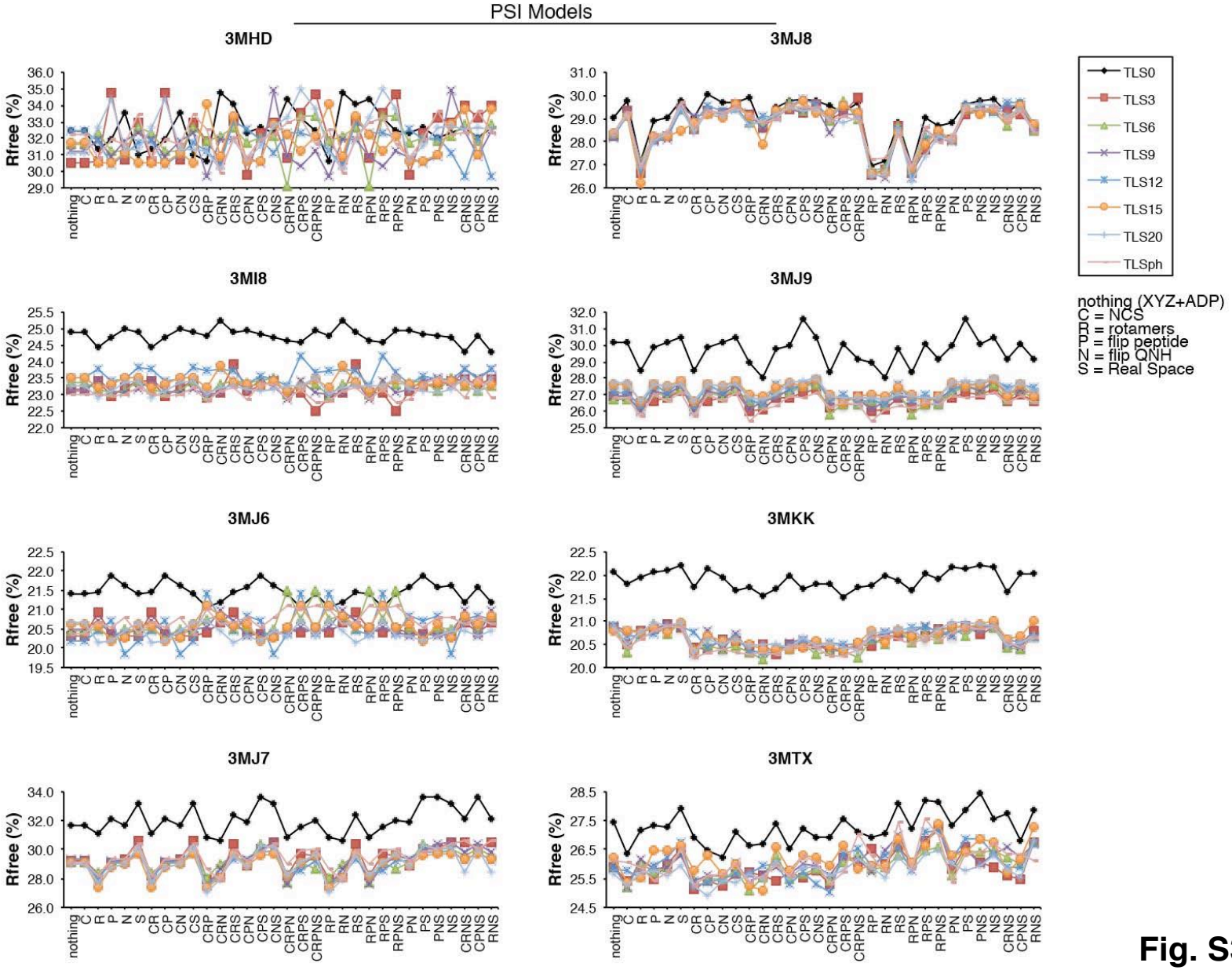
PSI Models
3MHD
3MJ8
3MI8
3MJ9
3MJ6
3MKK
3MJ7
3MTX
Rfree (%)
TLS0
TLS3
TLS6
TLS9
TLS12
TLS15
TLS20
TLSph
nothing (XYZ+ADP)
C = NCS
R = rotamers
P = flip peptide
N = flip QNH
S = Real Space

Fig. S3-2

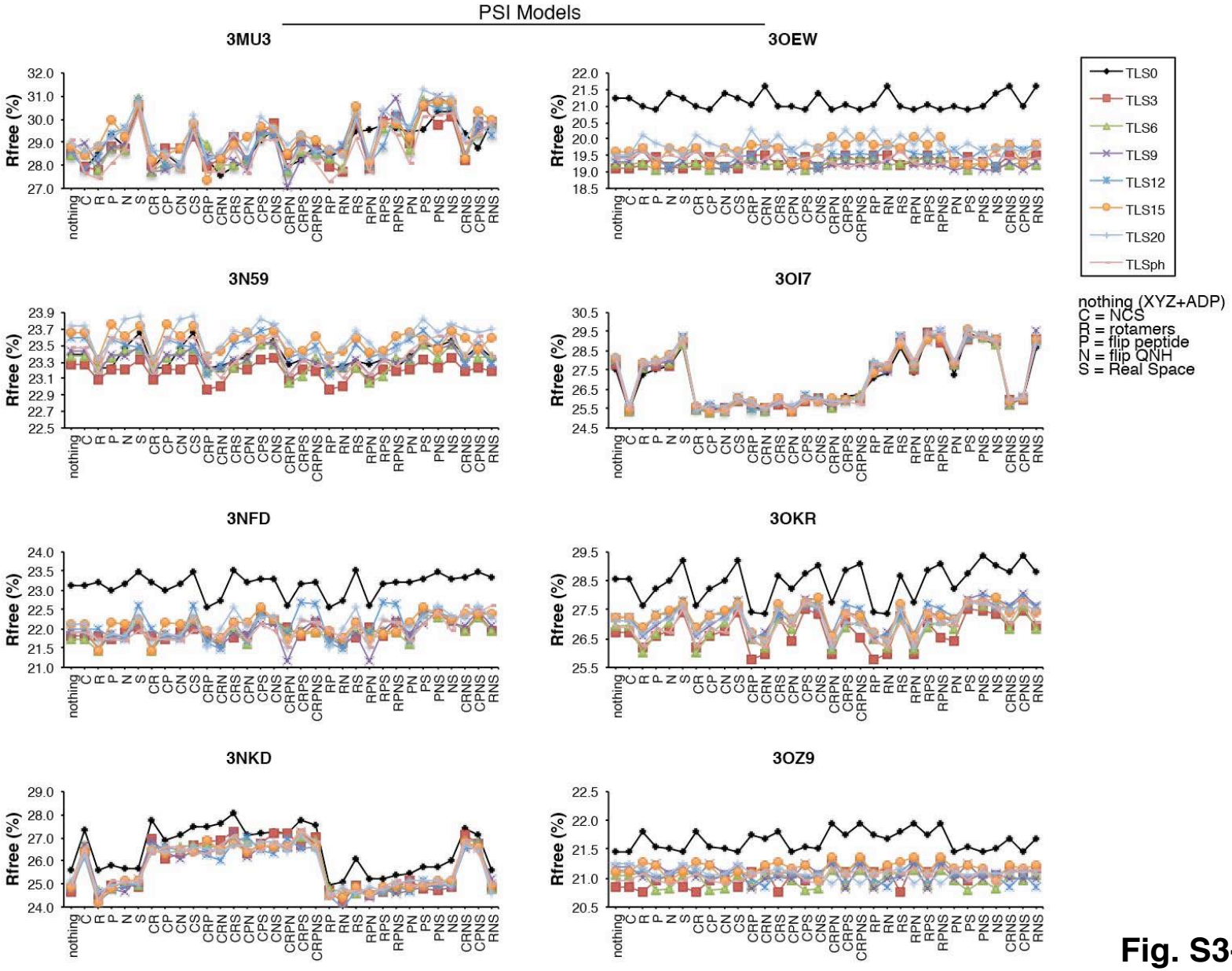
PSI Models
3MU3
3OEW
3N59
3OI7
3NFD
3OKR
3NKD
3OZ9
Rfree (%)
TLS0
TLS3
TLS6
TLS9
TLS12
TLS15
TLS20
TLSph
nothing (XYZ+ADP)
C = NCS
R = rotamers
P = flip peptide
N = flip QNH
S = Real Space

Fig. S3-3

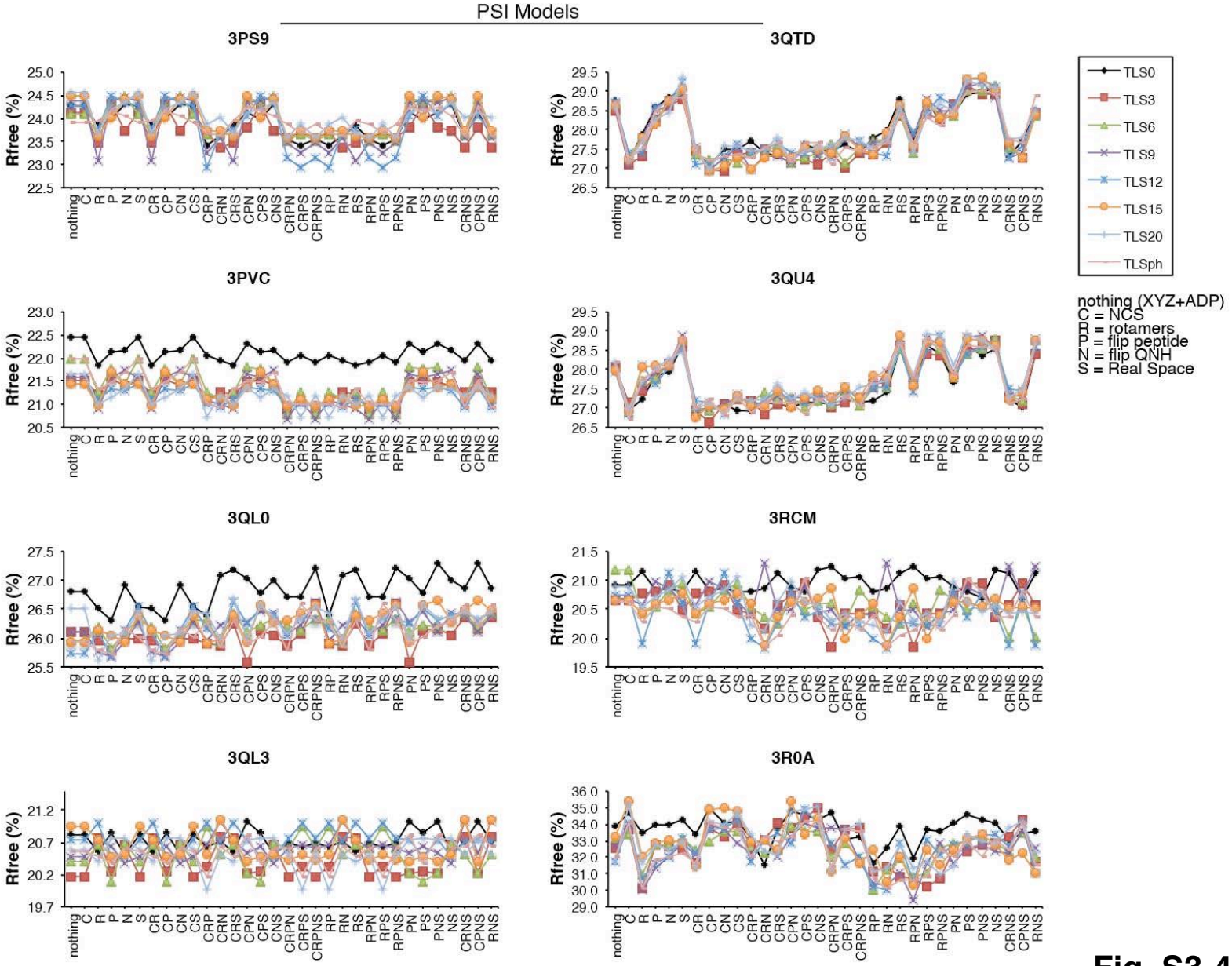
PSI Models
3PS9
3QTD
3PVC
3QU4
3QL0
3RCM
3QL3
3R0A
Rfree (%)
TLS0
TLS3
TLS6
TLS9
TLS12
TLS15
TLS20
TLSph
nothing (XYZ+ADP)
C = NCS
R = rotamers
P = flip peptide
N = flip QNH
S = Real Space

Fig. S3-4

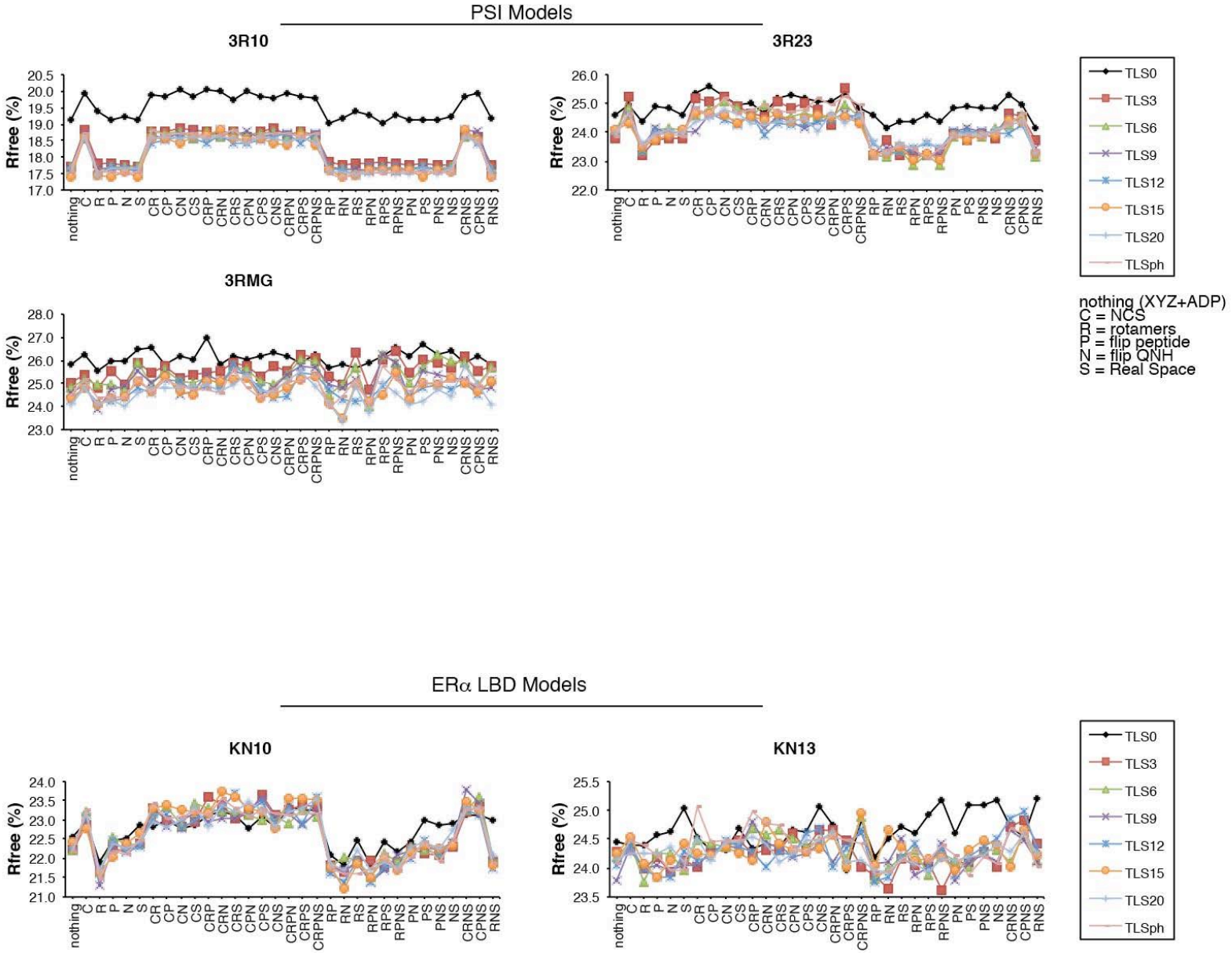
PSI Models
3R10
3R23
3RMG
Rfree (%)
nothing
C
R
P
N
S
CR
CP
CN
CS
CRP
CRN
CRS
CPN
CPS
CNS
CRPN
CRPS
CRPNS
RP
RN
RS
RPN
RPS
RPNS
PN
PS
PNS
NS
CRNS
CPNS
RNS
TLS0
TLS3
TLS6
TLS9
TLS12
TLS15
TLS20
TLSph
nothing (XYZ+ADP)
C = NCS
R = rotamers
P = flip peptide
N = flip QNH
S = Real Space
ERα LBD Models
KN10
KN13

Fig. S3-5

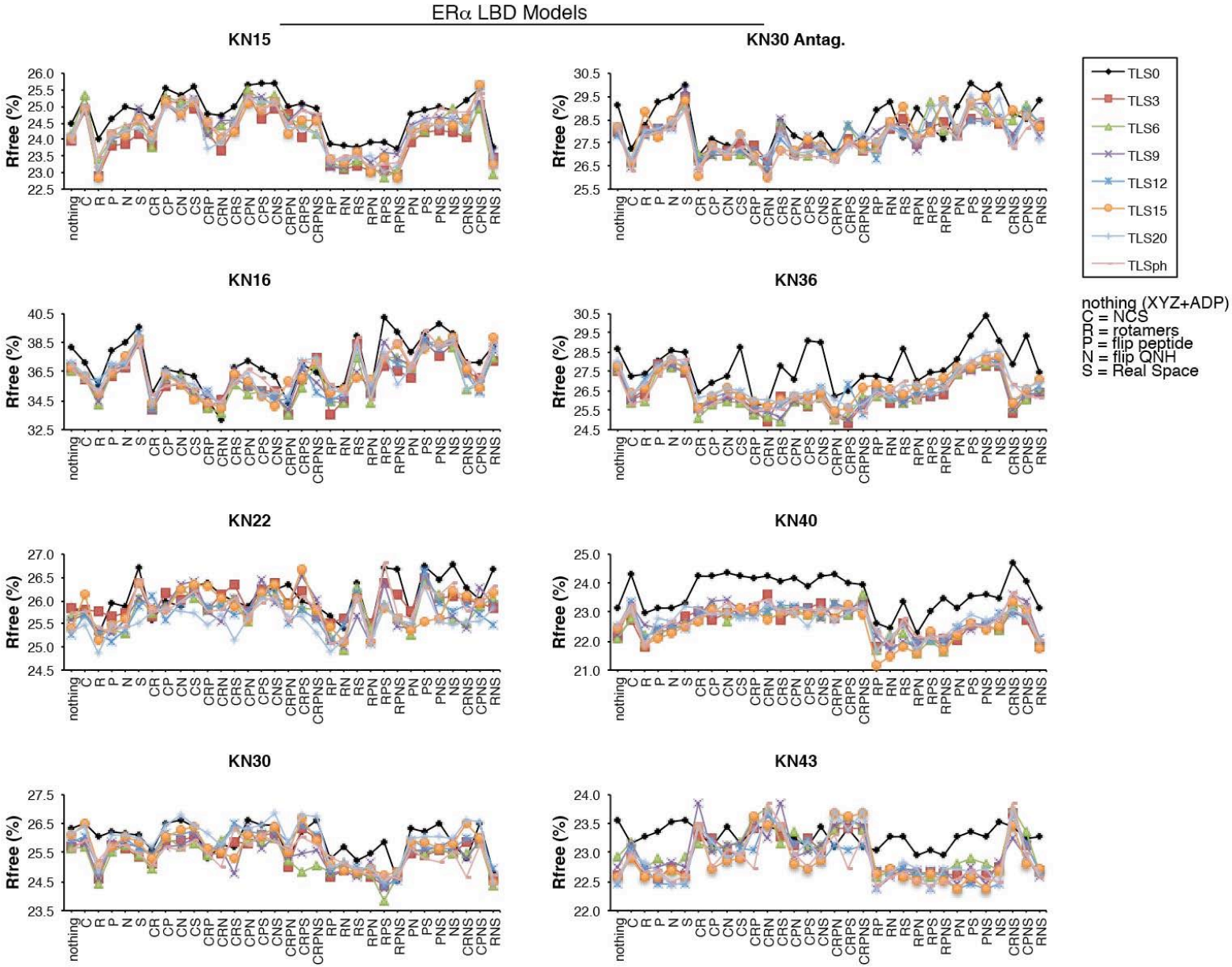
ERα LBD Models
KN15
KN30 Antag.
KN16
KN36
KN22
KN40
KN30
KN43
Rfree (%)
nothing
C
R
P
N
S
CR
CP
CN
CS
CRP
CRN
CRS
CPN
CPS
CNS
CRPN
CRPS
CRPNS
RP
RN
RS
RPN
RPS
RPNS
PN
PS
PNS
NS
CRNS
CPNS
RNS
TLS0
TLS3
TLS6
TLS9
TLS12
TLS15
TLS20
TLSph
nothing (XYZ+ADP)
C = NCS
R = rotamers
P = flip peptide
N = flip QNH
S = Real Space

Fig. S3-6

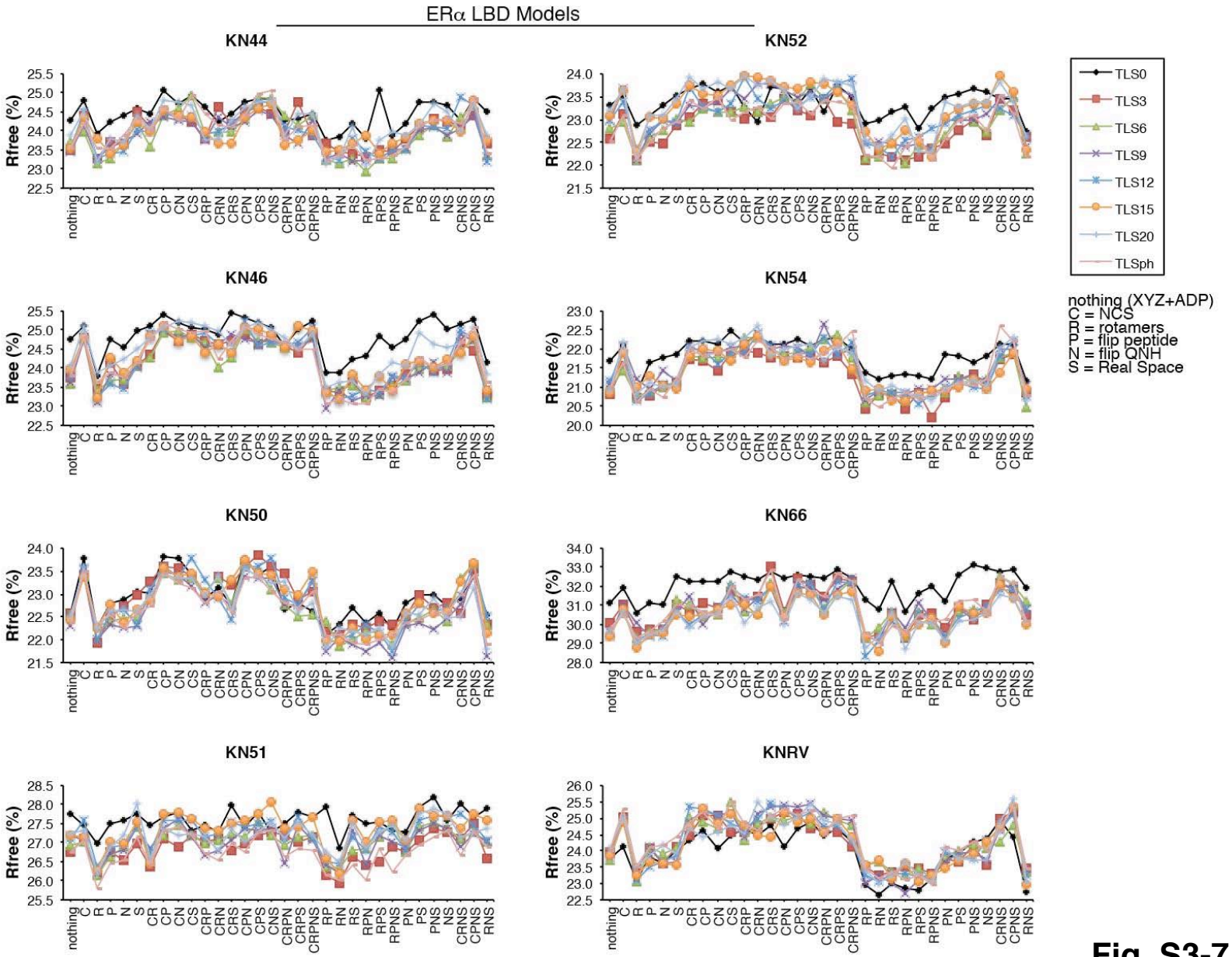
ERα LBD Models
KN44
KN52
KN46
KN54
KN50
KN66
KN51
KNRV
Rfree (%)
nothing
C
R
P
N
S
CR
CP
CN
CS
CRP
CRN
CRS
CPN
CPS
CNS
CRPN
CRPS
CRPNS
RP
RN
RS
RPN
RPS
RPNS
PN
PS
PNS
NS
CRNS
CPNS
RNS
TLS0
TLS3
TLS6
TLS9
TLS12
TLS15
TLS20
TLSph
nothing (XYZ+ADP)
C = NCS
R = rotamers
P = flip peptide
N = flip QNH
S = Real Space

Fig. S3-7

Figure S4, related to Figure 4

(**A**) Changes in the number of TLS groups induced a wide range of R_{free} values indicating models of varied quality. For each structural genomics data set, the effects of TLS on the range of R_{free} are plotted for each of the other 32-parameter sets following ExCoR. TLS column indicates the overall effects of TLS, while TLS# shows the effects of changing the number of TLS groups. The top dotted line shows the overall range of R_{free} for the full 256 ExCoR set. The bottom dotted line shows the range in R_{free} in the control refinement from implementing 2 new R_{free} test sets, as a rough measure of the noise in the refinements.

(**B**) Effects of TLS on 3MJ9 model statistics. Results of refinements performed using the parameter files shown in panel B, are shown. Using TLS refinement led to lower R-free, R-work, RMSD from ideal bonds and angles, Rotamer outliers, Ramachandran allowed and outliers, and Mol probity clashscore.

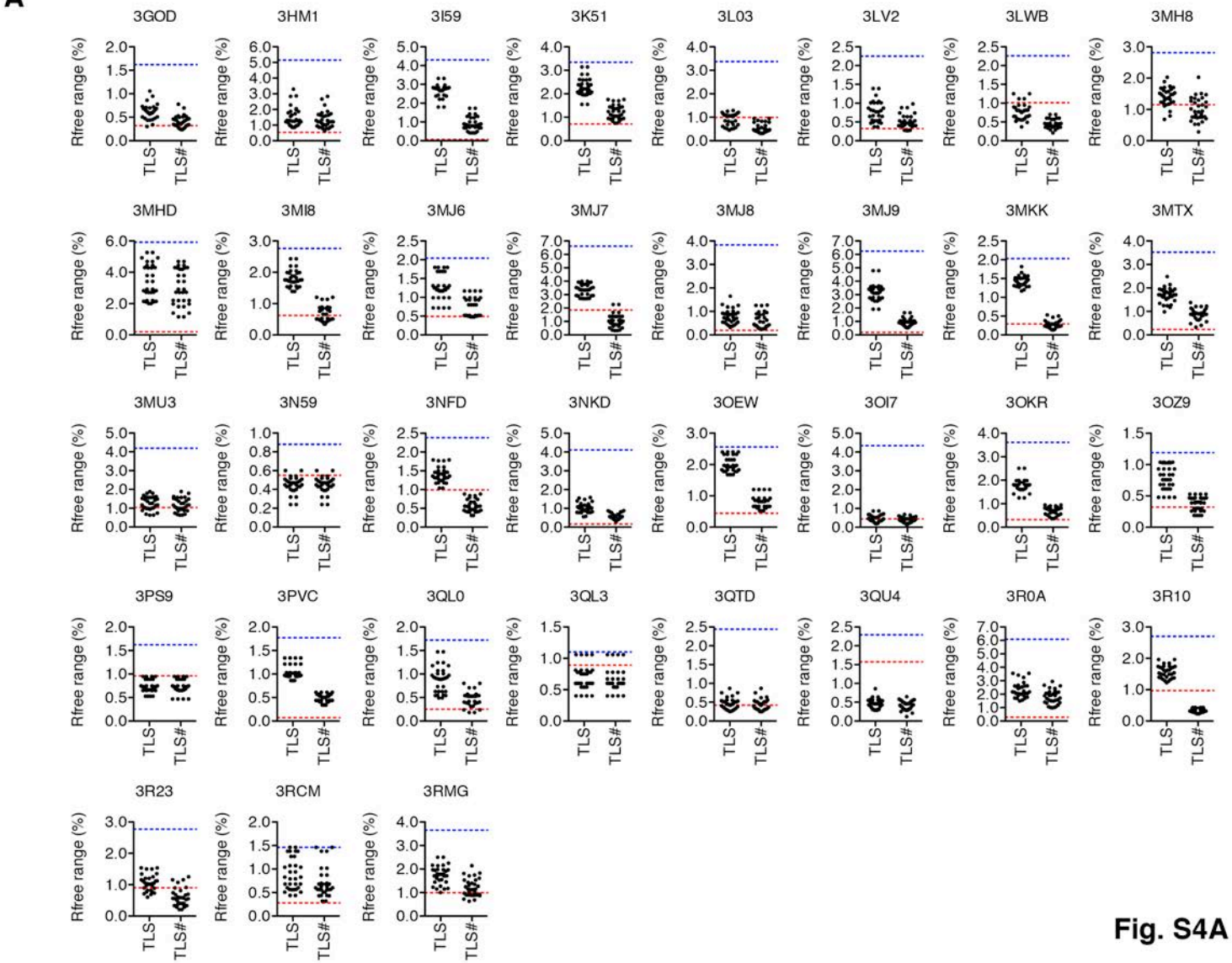
A
3GOD
3HM1
3I59
3K51
3L03
3LV2
3LWB
3MH8
3MHD
3MI8
3MJ6
3MJ7
3MJ8
3MJ9
3MKK
3MTX
3MU3
3N59
3NFD
3NKD
3OEW
3OI7
3OKR
3OZ9
3PS9
3PVC
3QL0
3QL3
3QTD
3QU4
3R0A
3R10
3R23
3RCM
3RMG
Rfree range (%)
TLS
TLS#

Fig. S4A

B

Refinement Statistics	Without TLS	With TLS
R-free	0.2917	0.2526
R-work	0.1934	0.1823
RMSD bonds	0.009	0.006
RMSD angles	1.41	1.07
Ramachandran allowed	11.003	9.871
Ramachandran outliers	5.502	2.265
Rotamer outliers	14.763	6.503
Average B	80.1	85.5
Clashscore	71.421	53.050

Fig. S4B

Table S1, related to Figure 3

Effects of ExCoR on 35 recently deposited structural genomics models and newly solved structures of the estrogen receptor ligand-binding domain in complex with different ligands

PDB ID	Res (Å)	R_{free} (%)		Rmsd bonds (Å)		Rmsd angles (°)		Average B		Wilson B
		ExCoR	Start[a]	ExCoR	Start	ExCoR	Start	ExCoR	Start	
3GOD	2.17	23.66	25.51	0.003	0.018	0.673	1.664	31.0	31.9	27.4
3HM1	2.33	26.55	29.16	0.003	0.008	1.048	1.573	66.1	70.7	39.6
3I59	2.29	26.17	28.49	0.003	0.022	0.795	1.950	73.0	73.0	55.1
3K51	2.45	21.11	24.91	0.004	0.028	0.854	0.822	68.7	79.1	44.6
3L03	1.90	20.24	22.77	0.003	0.014	1.050	1.790	46.8	44.8	31.5
3LV2	2.18	20.23	22.62	0.003	0.011	0.810	1.254	31.6	27.3	29.3
3LWB	2.10	21.50	22.14	0.007	0.005	1.068	1.104	44.7	45.9	34.2
3MH8	2.00	25.03	27.93	0.003	0.008	0.833	1.152	52.4	49.7	41.7
3MHD	2.90	29.07	34.65	0.003	0.011	1.054	1.265	130.8	147.3	78.3
3MI8	2.95	23.38	26.72	0.011	0.008	1.415	1.116	91.6	87.5	76.0
3MJ6	2.19	19.85	21.88	0.008	0.016	1.198	1.694	40.9	37.6	34.0
3MJ7	2.80	27.00	28.21	0.005	0.011	1.315	1.315	85.1	68.2	63.2
3MJ8	2.94	26.22	28.21	0.003	0.006	0.695	0.957	59.8	54.7	56.5
3MJ9	2.95	25.39	28.80	0.005	0.007	0.985	1.057	83.4	77.2	75.9
3MKK	1.91	20.18	25.79	0.006	0.015	1.090	1.424	29.2	9.6	23.1
3MTX	2.00	24.90	29.71	0.004	0.019	1.491	1.993	44.7	37.0	29.6
3MU3	2.40	27.06	28.98	0.007	0.021	1.256	1.970	36.4	32.0	33.6
3N59	2.52	22.97	24.93	0.003	0.006	0.682	0.905	41.0	37.5	38.0
3NFD	1.89	21.16	27.64	0.006	0.020	0.989	1.930	28.4	26.0	21.5
3NKD	1.95	23.95	26.94	0.003	0.022	0.728	1.691	39.2	33.8	28.3
3OEW	2.20	19.03	21.24	0.008	0.012	1.142	1.343	45.4	43.1	41.4
3OI7	2.40	25.28	26.20	0.004	0.013	0.850	1.394	26.8	23.9	25.8
3OKR	2.40	25.78	27.62	0.005	0.009	0.974	1.258	69.6	68.7	57.6
3OZ9	1.60	20.75	23.34	0.003	0.006	0.840	1.074	21.3	19.6	13.2
3PS9	2.54	22.94	24.54	0.004	0.012	0.868	1.481	26.4	22.5	24.6
3PVC	2.31	20.69	23.37	0.004	0.026	1.024	1.756	30.8	25.9	25.3
3QL0	1.60	25.58	27.14	0.010	0.014	1.572	1.597	19.8	19.3	14.3
3QL3	1.80	19.95	22.15	0.009	0.017	1.576	1.601	17.8	16.4	12.9
3QTD	2.70	26.91	28.58	0.003	0.024	0.728	1.739	38.8	32.5	33.4
3QU4	2.10	26.64	29.36	0.004	0.009	0.876	1.173	37.3	36.2	30.1
3R0A	2.30	29.36	34.85	0.003	0.014	0.829	1.497	63.9	51.3	49.2
3R10	2.00	17.83	19.07	0.006	0.008	0.942	1.199	25.5	20.3	20.1
3R23	2.50	23.02	25.51	0.002	0.012	0.639	1.518	56.1	44.9	40.2
3RCM	2.05	19.83	25.56	0.003	0.014	0.740	1.449	22.1	18.4	17.6

3RMG	2.30	23.35	26.80	0.003	0.010	0.692	1.093	77.5	67.6	46.7

ER LBD Model	Res (Å)	R_{free} (%)			Rmsd bonds (Å)			Rmsd angles (°)		
		ExCoR	Control	Start	ExCoR	Control	Start	ExCoR	Control	Start
KN10	2.24	21.22	22.58	25.63	0.003	0.003	0.027	0.645	0.640	1.635
KN13	2.24	23.62	24.45	26.51	0.004	0.003	0.014	0.793	0.655	1.327
KN15[c]	2.24	22.83	24.46	26.00	0.003	0.002	0.016	0.709	0.595	1.591
KN16*	2.16	33.19	38.17	37.97	0.010	0.003	0.029	1.471	0.796	2.590
KN22	1.93	24.86	25.89	26.90	0.003	0.002	0.026	0.692	0.551	2.427
KN30*	2.33	25.99	29.10	27.50	0.037[b]	0.020	0.022	2.662[b]	2.784	1.935
KN30	2.25	23.82	26.36	27.33	0.010	0.014	0.018	1.643	1.940	1.758
KN36	2.38	24.98	27.98	27.57	0.048[b]	0.013	0.019	3.248[b]	2.149	1.894
KN40[c]	1.93	21.19	23.13	25.86	0.004	0.003	0.028	0.766	0.652	1.555
KN43	2.24	22.35	23.57	23.92	0.003	0.003	0.007	0.630	0.603	0.961
KN44	2.24	22.94	24.26	25.25	0.003	0.005	0.014	1.204	0.791	1.382
KN46	2.24	22.94	24.74	26.61	0.003	0.003	0.026	0.706	0.625	1.461
KN50	2.24	21.59	22.59	24.27	0.003	0.003	0.013	0.602	0.599	1.368
KN51	2.24	25.81	27.74	28.27	0.003	0.002	0.013	0.715	0.571	1.416
KN52	2.24	21.93	23.32	24.71	0.002	0.002	0.013	0.544	0.504	1.302
KN54	1.93	20.23	21.69	23.57	0.004	0.003	0.010	0.711	0.664	1.172
KN66	1.98	28.33	31.14	34.57	0.004	0.002	0.019	0.878	0.584	1.802
KNRV	2.20	22.66	23.74	26.92	0.003	0.002	0.018	0.679	0.619	1.642

*Antagonist-bound conformation

[a] Statistics for each model starting downloaded from the PDB were re-calculated and used as a control.

[b] Unusually high RMSD values likely due to receptor conformation, NCS, ligand-receptor dynamics, and/or inadequate ligand restraints.

[c] ER LBD models KN15 (PDB ID: 4IWC) and KN40 (PBD ID: 4IWF) were later completed and published elsewhere while this manuscript was under review. Other ER LBD models will be completed and published elsewhere.

Supplemental References

Lovell, S.C., Word, J.M., Richardson, J.S., and Richardson, D.C. (2000). The penultimate rotamer library. Proteins *40*, 389-408.

Word, J.M., Lovell, S.C., Richardson, J.S., and Richardson, D.C. (1999). Asparagine and glutamine: using hydrogen atom contacts in the choice of side-chain amide orientation. J Mol Biol *285*, 1735-1747.